

## VIBRATIONAL SPECTRA OF (HF)<sub>2</sub>, (HF)<sub>n</sub> AND THEIR D-ISOTOPOMERS: MODE SELECTIVE REARRANGEMENTS AND NONSTATISTICAL UNIMOLECULAR DECAY

Katharina VON PUTTKAMER and Martin QUACK

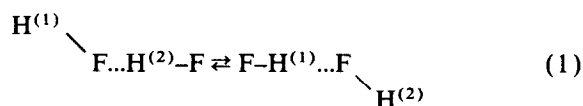
*Laboratorium für Physikalische Chemie, ETH Zürich (Zentrum), CH-8092 Zurich, Switzerland*

Received 18 May 1989

We have measured a complete survey of the rovibrational spectrum of gaseous hydrogen fluoride and its D-isotopomers under equilibrium conditions from the far infrared (low-frequency fundamentals of (HF)<sub>2</sub>) to the visible (*N*=4 overtones of the HF stretching vibrations in (HF)<sub>n</sub>) by interferometric Fourier transform spectroscopy. The data have been analyzed in terms of the tunneling splittings for the hydrogen bond rearrangements (H<sup>(1)</sup>-F...H<sup>(2)</sup>-F) ⇌ (F-H<sup>(1)</sup>...F-H<sup>(2)</sup>), which are highly mode specific. Furthermore, narrow line structure is observed for the HF stretching fundamentals and overtones in (HF)<sub>2</sub> from *N*=1 to *N*=4. These are found to be inconsistent with quasi-equilibrium (RRKM) theories of unimolecular dissociation. Simplified coupled channel calculations by Halberstadt et al. predict lifetimes that are reasonably consistent with experiment. The results are discussed in terms of an adiabatic separation of the two high-frequency HF stretching modes and the four low-frequency modes in (HF)<sub>2</sub>.

### 1. Introduction

The dynamics of hydrogen bond formation and breaking is of fundamental importance for the understanding of biophysical–chemical primary processes and of condensation and evaporation phenomena in hydrogen bonded liquids [1–3]. There is a surprising lack of knowledge of even the simplest dynamical processes such as the detailed kinetics of dimer formation as the first step in the condensation of hydrogen bonded liquids or the reverse dissociation (evaporation) process. Whereas water would be obviously one of the most important practical systems for investigation [3], hydrogen fluoride is attractive for model studies because of its greater simplicity, still sharing all the important features with other prototype hydrogen bonded systems. For the hydrogen fluoride dimer we can formulate the two kinetic primary processes of the exchange of the hydrogen bridge proton:



and of the unimolecular dissociation of the hydrogen bond:



The first is a typical isomerization reaction of a non-rigid molecule (an observable isotopomerisation, if there is isotope labeling). The second is a “vibrational predissociation” [4,5] or simple bond fission reaction on a single electronic potential surface [6]. Both processes occur in a more complex fashion also in larger hydrogen bonded clusters. Energetically and dynamically the hydrogen bond is situated between simple van der Waals bonds [7] and ordinary chemical bonds. Obvious first questions concern thus the quantitative description of the processes (1) and (2) and, in particular, whether quasi-equilibrium statistical theories of unimolecular reaction might be applicable [8] or whether highly nonequilibrium non-statistical behaviour is observed, perhaps including mode selective effects [9,10]. These questions can be addressed by high-resolution molecular spectroscopy, which is the aim of the present investigation.

Early work on the vibrational spectra of hydrogen fluoride vapour has been restricted to studies without rotational line resolution for the dimer or higher polymers sometimes in matrices [1–3,11–20]. By such studies some vibrational frequencies and the chemical equilibria [21,22] could be partially char-

acterized. Prior to our studies, rotational resolution had been achieved only in the pioneering microwave investigations [23–29] and in laser spectroscopy of the HF stretching fundamental vibrations of the dimer [30–41]. We have previously reported the far infrared rotational spectrum [42] and a first analysis of the low-frequency out of plane bending fundamental [43,44]. Preliminary accounts of our investigations of HF stretching overtone predissociation spectra have appeared [45,46]. In a more general spectroscopic context one may mention the claim of the observation of bending vibrational transitions in the trimer (HF)<sub>3</sub> [47] and the investigations of the symmetry group of nonrigid (HF)<sub>2</sub> [48–50]. There have been numerous *ab initio* investigations of the ground state potential surface of the HF dimer [51–63]. (This list is incomplete, for further references see these papers and refs. [1,26,44].) There has also been some discussion concerning the hydrogen bond dissociation energy of (HF)<sub>2</sub> and (HF)<sub>n</sub> [21,22,64,65], but this seems to be now well established at  $\Delta H_0^0 \equiv D_0^0 = 12.7 \text{ kJ mol}^{-1}$  [32,40]. A variety of theoretical models and calculations of predissociation rates have appeared [66–78]. Our experimental results provide evidence concerning the validity of these and others.

## 2. Experimental

All spectra have been recorded on our BOMEM DA.002 interferometric Fourier transform spectrometer system. The Michelson interferometer has a maximum mirror displacement of 1.25 m and correspondingly an optimum instrument function of width  $0.004 \text{ cm}^{-1}$  (fwhm, apodized,  $0.0024 \text{ cm}^{-1}$  unapodized) and a resolving power  $\bar{\nu}/\Delta\bar{\nu} > 10^6$ . Actual linewidths were usually governed by pressure broadening. For the various spectral ranges a variety of optical components have been used as described previously [43,44,79,80]. We have used two types of long path thermostatted cells built in our laboratory. For safety reasons the inner cell diameter was restricted to 4 cm, in order to avoid handling too large quantities of HF. This implies certain optical losses. With the arrangement shown in fig. 1 the transmission was  $< 20\%$  with double pass through the cells (4 or 10 m optical path length, respectively). The cells were of steel (V2A or

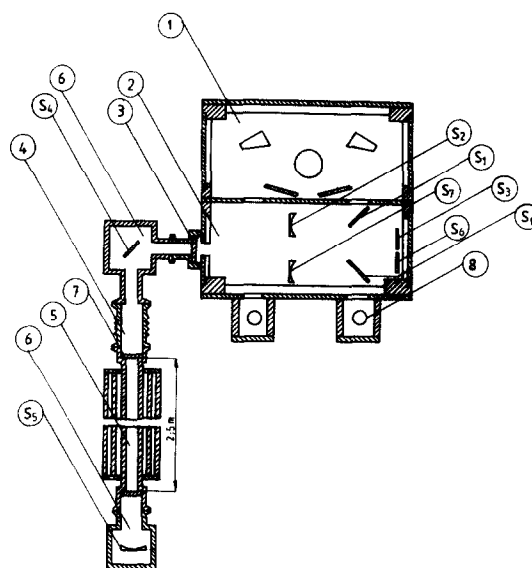
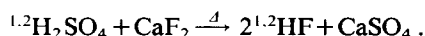


Fig. 1. Drawing of the optical setup (top view). (1) is the interferometer (moving mirror perpendicular to the plane at circle 0) showing the transfer optics to an evacuated chamber (2) with mirrors  $S_1, S_3, S_6, S_8$  (flat) and  $S_2, S_7$  ( $f=0.125 \text{ m}$ ). This is normally the sample chamber but here it contains the transfer optics to the coolable cell (5), via flat mirror  $S_4$ , reflection at  $S_5$  ( $f=2$  or  $5 \text{ m}$ ). (6) are separately evacuated safety chambers. (3) and (7): windows, (4): flexible part, (8): detector. The cell length can be 2 m or 5 m, alternatively.

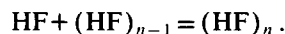
AISI304 for the 2 m cell and V4A or AISI316 for the 5 m cell, the latter showing substantially less corrosion by HF). The cell windows were of  $\text{CaF}_2$  or polyethylene in the mid-near IR or far IR respectively. The cells were totally separated from the interferometer and optics by an evacuable safety chamber, from which in case of leaks HF could be removed and destroyed automatically by the reaction  $2\text{HF} + \text{CaO} \rightarrow \text{CaF}_2 + \text{H}_2\text{O}$ . The gas handling and vacuum system was made of stainless steel and monel (Ni/Cu) and used stainless steel fittings (Swagelok) and teflon or viton gaskets. The cell windows were heated to room temperature and thermally isolated from the cell by teflon. The temperatures were measured with thermoelements in direct contact with the gas in the middle and at the ends of the cell. Over 4 m length there was no measurable  $T$  gradient in the 5 m cell (control to  $< 1 \text{ K}$ ), whereas near the windows temperatures rose by about 5 K. Pressures were measured by MKS Baratron and Keller manometers,

which have been calibrated in our laboratory against a manometer calibrated by the Amt für Messwesen, Bern.

HF was obtained from Matheson and Merck (Darmstadt). It contained some non-condensable, non-absorbing components (presumably air). We furthermore prepared samples of HF and DF in our laboratory by



There were generally no appreciable impurities. In a few cases some SiF<sub>4</sub> could be detected, which presumably was generated by reaction of HF with parts of the system which were not identified with certainty. Equilibria were estimated using data from ref. [64]



We usually tried to work at temperatures and pressures optimizing both the mole fraction of (HF)<sub>2</sub> and limiting the effects of pressure broadening. Mole fractions in the range 0.01–0.05 can be achieved rather easily. The new dissociation energy  $\Delta H_0^0 = 12.740 \text{ kJ mol}^{-1}$  for (HF)<sub>2</sub> [40] would change the predicted equilibrium concentration somewhat, but large uncertainties remain anyway.

### 3. Results

#### 3.1. Survey of the fundamental and overtone spectrum in (HF)<sub>n</sub> and (DF)<sub>n</sub>

Fig. 2 shows a summary of spectra of hydrogen fluoride between 2500 and 15000 cm<sup>-1</sup>. One can recognize the rotational line structure from the monomer and from DF in natural abundance (perhaps slightly increased). For the higher overtones the R-branch band head becomes increasingly pronounced. Within the monomer line structure one finds the fine structure from dimer absorption, which looks like noise on that scale, but true noise is negligible in these spectra. Much more shifted to lower wavenumbers in each band one finds the continuous absorption from polymers with  $n > 2$ . Even at the highest resolution there is no fine structure visible in these bands under the conditions of our experiments. Because of the rel-

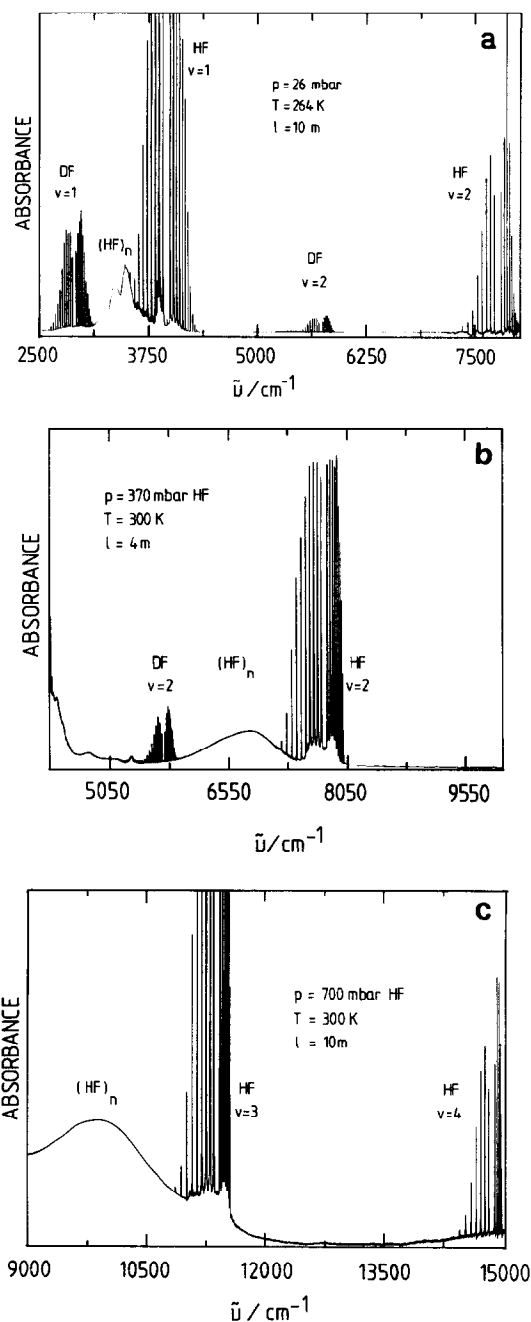


Fig. 2. Survey of the IR absorption spectrum of natural HF, (HF)<sub>n</sub>. (a) 2500–8000 cm<sup>-1</sup>, 26 mbar, 10 m, 264 K,  $\Delta\bar{\nu} = 0.5 \text{ cm}^{-1}$ , absorbance range 0–5. (b) 4300–10000 cm<sup>-1</sup>, 370 mbar, 300 K, 4 m,  $\Delta\bar{\nu} = 0.3 \text{ cm}^{-1}$ , absorbance range 0–4. (c) 9000–15000 cm<sup>-1</sup>, 700 mbar, 300 K, 10 m,  $\Delta\bar{\nu} = 0.7 \text{ cm}^{-1}$ , absorbance range 0–0.5.

atively large pressure broadening and severe hot band congestion this does not prove the absence of structure. One notes a substantial intensity for these polymer absorptions. In the region of the fundamental the maximum is close to the one observed in the absorption of liquid HF ( $3400\text{ cm}^{-1}$ ) but the double peak structure is characteristic of the vapour. Similar spectra are observed for HF/DF mixtures and for DF, as shown for the examples in fig. 3. Fig. 4 illustrates the pressure dependence of the spectrum, with an increasing mole fraction of the higher polymers as  $p$  increases. In the course of our investigations we have obtained some new results even on the well studied monomers, as for  $\nu=3$  and 4 of DF there seem to exist no direct measurements, yet. A spectrum is shown in fig. 5, and table 1 summarizes the band origins obtained in the present work compared to earlier re-

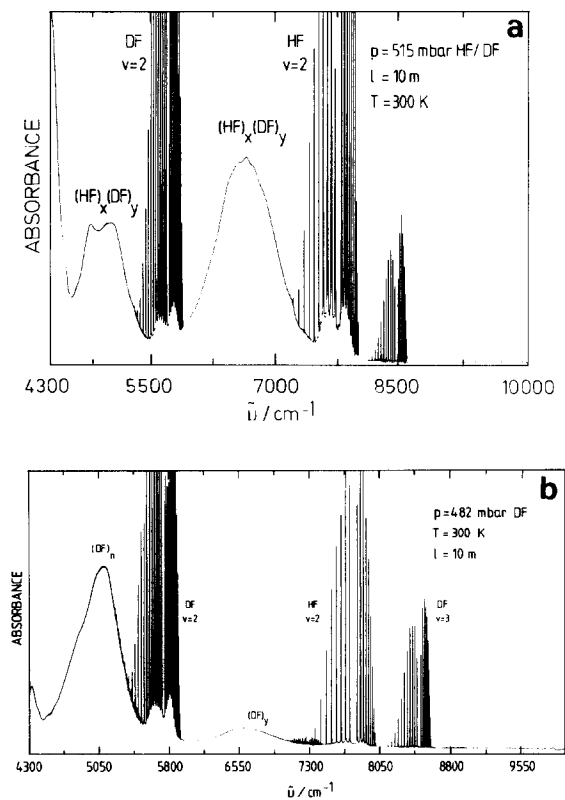


Fig. 3. Survey spectrum of HF isotopomers  $4300\text{--}10000\text{ cm}^{-1}$ . (a) 515 mbar HF/DF (1/1) mixture, 300 K, 10 m,  $\Delta\tilde{\nu}=0.3\text{ cm}^{-1}$ , absorbance range 0–5. (b) 482 mbar DF (with HF impurity), 300 K, 10 m,  $\Delta\tilde{\nu}=0.3\text{ cm}^{-1}$ , absorbance range 0–5.

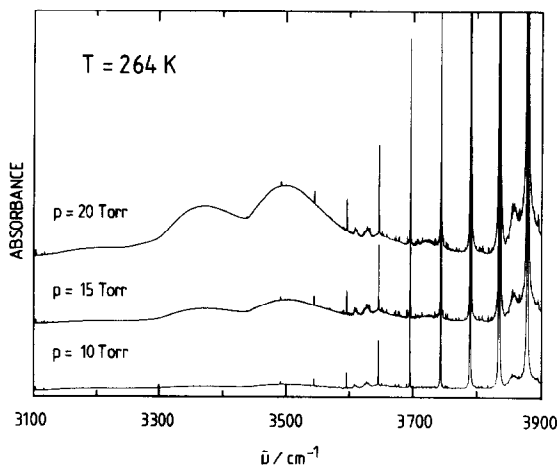


Fig. 4. Pressure dependence of the spectrum in the range of HF stretching fundamentals of  $(\text{HF})_n$  at 264 K and pressures as indicated ( $l=10\text{ m}$ ,  $\Delta\tilde{\nu}=0.5\text{ cm}^{-1}$ , absorbance range 0–5).

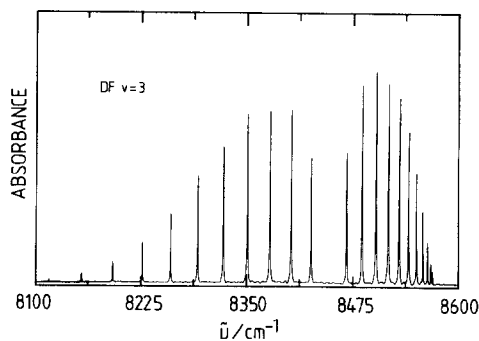


Fig. 5. Spectrum of DF monomer ( $\nu=3$ ), 482 mbar, 298 K, 10 m,  $\Delta\tilde{\nu}=0.3\text{ cm}^{-1}$ , absorbance range 0–4.

sults, where available. We note that our new experimental results for DF improve significantly upon values predicted on the basis of Dunham parameters [81–85].

The assignment of band centers for the dimer absorptions is discussed in detail in the subsections 3.2 and 3.3. For the purpose of best comparison with the monomer absorption the results are summarized here in table 2. For the overtones the results are crude estimates (particularly for  $n\nu_2$ ), as a full analysis of the rotational structure was not possible. The comparison with the monomer shows, nevertheless, that both  $n\nu_1$  and  $n\nu_2$  in the dimer are shifted towards low

Table 1  
Band centers for vibrational bands of HF and DF

$\nu$	$\bar{\nu}$ (cm <sup>-1</sup> )		Ref.
	HF	DF	
1	3961.42290(25) 3961.4231(6)	2906.6610(12)	[81,82] this work
2	7750.7949(15) 7750.7938(6)	5721.815(5)	[81,84] this work
3	11372.807(7) 11372.783(2)	- 8447.3835(47)	[83] this work <sup>a)</sup>
4	14831.627(7) 14831.630(8)	- 11085.014(23)	[83] this work <sup>b)</sup>

<sup>a)</sup> DF,  $B_3=9.9876(2)$  cm<sup>-1</sup>,  $D_3=0.5521(16)\times 10^{-3}$  cm<sup>-1</sup>,  $H_3=22.8(50)\times 10^{-9}$  cm<sup>-1</sup>, constrained to  $H_0$  [82].

<sup>b)</sup> DF,  $B_4=9.7065(18)$  cm<sup>-1</sup>,  $D_0=0.514(27)\times 10^{-3}$  cm<sup>-1</sup>,  $H_3=H_0$  constrained; calibrations were performed with water lines and HF lines.

Table 2  
HF stretching fundamentals and overtones for (HF)<sub>2</sub>

$\nu$	$\bar{\nu}_1$ (cm <sup>-1</sup> )	$\bar{\nu}_2$ (cm <sup>-1</sup> )	Notes
1	3930.7	3867.9	this work and ref. [31]
2	7700 ± 20	7555 ± 15	estimate, this work
3	11260	11060	estimate (section 3.3)
4	14650	14400	estimate (section 3.3)

wavenumbers from the monomer absorptions. In spite of the uncertainty of the band center estimates it must be emphasized that in all cases absorption features were identified that clearly belonged to (HF)<sub>2</sub> overtones.

### 3.2. Rotational fine structure in the fundamentals and their associated combination and hot bands in (HF)<sub>2</sub>

Table 3 summarizes the fundamentals of (HF)<sub>2</sub> and their expected appearance depending on symmetry selection rules. Of the predicted bands, three are now known with a rotational analysis ( $\nu_1, \nu_2, \nu_6$ ). As (HF)<sub>2</sub> is a near symmetric top, the coarse band structure can be characterized as either parallel ( $\parallel$ ,  $\Delta K_a=0$ ) or perpendicular ( $\perp$ ,  $\Delta K_a=\pm 1$ ) with respect to the near symmetry axis “*a*” (about F...H-F axis, the asymmetry parameter is  $\kappa = -0.9998$ ). The rovibrational levels are split by tunneling (process (1)) by an amount which is small but detectable for

most fundamentals. Only for the tunneling motion  $\nu_5$  it is large and we have given in table 3 the lower tunneling component. For the A<sup>+</sup> vibrations, the IR transitions connect the lower (upper) tunneling level in the vibrational ground state with the upper (lower) tunneling level in the excited state. For the B<sup>+</sup> and A<sup>-</sup> vibrations in both states only the lower or the upper tunneling levels combine, with further differences of selection rules for the rotational levels (overall rovibronic selection rule A<sup>+</sup> ↔ A<sup>-</sup> and B<sup>+</sup> ↔ B<sup>-</sup>). The situation has been analyzed in detail by Hougen and Ohashi [50] for the relevant trans tunneling path and discussed in ref. [44] in relation to our analysis of  $\nu_6$ . For the HF stretching fundamentals one expects two transitions, one mainly perpendicular (“antisymmetric stretching”  $\nu_1$ ) at high wavenumber, one dominantly parallel (“symmetric stretching”  $\nu_2$ ). Fig. 6 shows the survey of the HF stretching region, where one can very nicely identify the  $K=1\leftarrow 0$  transition of the former in the central gap of the monomer absorption near 3963 cm<sup>-1</sup> and the more complex features associated with the  $\Delta K=0$  transitions of  $\nu_2$  around 3868 cm<sup>-1</sup>. Although not obvious at the scale shown in fig. 6 these bands are quite strong and have been largely analyzed at very high resolution [30–33]. We have given a summary of these and also some new data in ref. [42].

Fig. 7 provides a survey of Q branches for  $\nu_1$ .  ${}^R Q_0$  in fig. 7a has been presented before at very high resolution by Pine and co-workers [30–33] under various conditions. Under the conditions in fig. 7 its line widths are determined by pressure broadening (0.02 cm<sup>-1</sup> with instrumental bandwidth=0.004 cm<sup>-1</sup>, fwhm). Compared to the  ${}^P Q$  branches shown in figs. 7b and 7c one notes a very small splitting in  ${}^R Q_0$  ( $\approx 0.312$  cm<sup>-1</sup>), which results in a smooth overall shape of the absorption, without easily visible tunneling splitting in a low-resolution view of the band. This small apparent splitting remains true for the higher  ${}^R Q_n$  branches. It is the result of two effects compensating each other: With increasing  $K$ , the tunneling splitting of levels increases, whereas it decreases for  $\nu_1=1$  compared to  $\nu_1=0$ . Indeed, the tunneling splitting for a level with  $\nu_1=0$ ,  $K=n$  is always fairly close to the one of the level with  $\nu_1=1$ ,  $K=n+1$ , and thus the transitions for the two tunneling components are always close. For the  ${}^P Q_n$  branches there is no such compensating effect and the splitting in the

Table 3  
Summary of vibrational transitions and selection rules

Vibration	$\Gamma_{\text{vib}}^{\text{a)}}$	Selection rule <sup>b)</sup>	$\bar{\nu}$ (cm <sup>-1</sup> )
$\nu_1$ (free) HF stretching	A', B <sup>+</sup>	$\perp, \Delta K_a = \pm 1$ , b type	3931 <sup>d)</sup>
$\nu_2$ (bound) HF stretching	A', A <sup>+</sup>	$\parallel, \Delta K_a = 0$ , a type	3868 <sup>d)</sup>
$\nu_3$ symmetric bending	A', A <sup>+</sup>	$\perp, \Delta K_a = \pm 1$ , b type	510 <sup>e)</sup>
$\nu_4$ F...F stretching	A', A <sup>+</sup>	$\parallel, \Delta K_a = 0$ , a type	150 <sup>e)</sup>
$\nu_5$ antisymmetric bending	A', A <sup>+</sup> (B <sup>+</sup> )	$\perp, \Delta K_a = \pm 1$ , b type	216 <sup>e)</sup> 161 <sup>f)</sup>
$\nu_6$ out of plane bending	A'', A <sup>-</sup>	$\perp, \Delta K_a = \pm 1$ , c type	370 <sup>e)</sup>

a) See ref. [44] for definitions of  $\Gamma_{\text{vib}}$  in M<sub>S4</sub>.

b) Approximate symmetric top selection rule, only dominant component, in practice hybrids are expected.

c) Estimated band center, the  $K=1 \leftarrow 0$  transition is at 400 cm<sup>-1</sup> [44]. The quantum Monte Carlo (ab initio) result gives an anharmonic wavenumber of 399 cm<sup>-1</sup> [102], the harmonic ab initio wavenumber is 413 cm<sup>-1</sup> [51].

d) Experiment, see table 2. e) Predicted [51] harmonic wave number.

f) Lower tunneling component predicted in ref. [53].

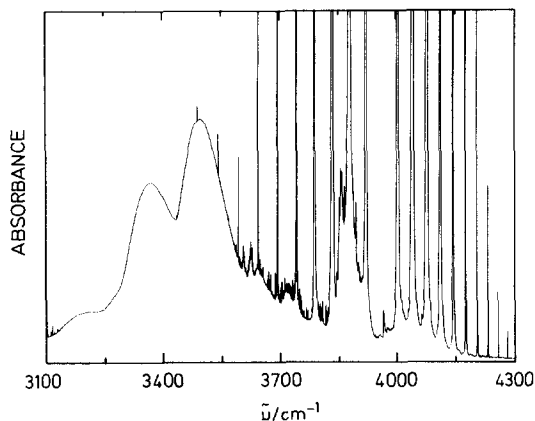


Fig. 6. Survey of HF stretching fundamental absorption in (HF)<sub>n</sub>. One recognizes the central <sup>R</sup>Q<sub>0</sub> (between P and R of HF) of (HF)<sub>2</sub>, weak but real peaks from <sup>P,R</sup>Q<sub>n</sub> (for instance <sup>R</sup>Q<sub>3</sub> at 4060) and  $\nu_2$  around 3850 cm<sup>-1</sup> (20 Torr, 265 K, 10 m,  $\Delta\bar{\nu} \approx 0.5$  cm<sup>-1</sup>, absorbance range 0–1.5).

bands rises in any easily visible manner from 0.85 to 3.1 cm<sup>-1</sup> (figs. 7b and 7c). The deep broad line in <sup>P</sup>Q<sub>3</sub> is probably due to a perturbation (the sharp, very deep lines in the experimental spectra are due to un-compensated water lines). For <sup>P</sup>Q<sub>4</sub> there is only one Q branch clearly visible (with very weak additional features at 3767.4 and above 3771 cm<sup>-1</sup>). As discussed before, also in the rotational spectrum, only the B<sup>+</sup> tunneling level of  $K=4$  could be located [42]. There is probably a complex perturbation occurring for the A<sup>+</sup> ( $K=4$ ) level, which removes simple, sharp

structures. This level is expected to be very close (377 to 383 cm<sup>-1</sup>?) to a band doublet observed in ref. [44] at 383.34 and 382.03 cm<sup>-1</sup> and also close to the position of  $\nu_6$  ( $K=0$ ) around 370 cm<sup>-1</sup>.

Fig. 8 shows the range of the expected <sup>R</sup>Q<sub>4</sub> and <sup>R</sup>Q<sub>5</sub> transitions. Here, too, only single sharp features at 4084 and 4105 cm<sup>-1</sup> can be seen. For the Q branch at 4084 cm<sup>-1</sup> a partial rotational analysis was possible, giving a band center at  $4083 \pm 2$  cm<sup>-1</sup>, with error limits arising from uncertainties in the  $J$  assignment.

For the rotational analyses of the various bands we have followed two approaches. In the first, each level with ( $\nu_1, \nu_2, \dots, \Gamma_{\text{tun}}, K_a$ ) is taken as giving a separate vibration–tunneling– $K_a$  rotation subband with a hypothetical band origin at  $J=0$  (the lowest real level occurs for  $J=K_a$ ). These levels would be obtained in a theoretical rotation–vibration model calculation in several dimensions, for instance by variational methods. The  $J$  dependence of energy levels is described by the usual term formulae

$$\begin{aligned}
 E_{\nu K}/hc = & \bar{\nu}_{\nu K} + (\bar{B}_{\nu K} \pm \frac{1}{4} \delta_{K1} b_{\nu K}) J(J+1) \\
 & - [D_{\nu K} \mp (\delta_{K1} + \delta_{K2}) d_{\nu K}] J^2(J+1)^2 \\
 & + (H_{\nu K} \pm \delta_{K2} h_{\nu K}) J^3(J+1)^3, \quad (3)
 \end{aligned}$$

$\bar{\nu}_{\nu K}$  is the subband origin for a given  $K$  level in the vibrational–tunneling state  $\nu$ .  $\bar{B}_{\nu K} = (B_{\nu K} + C_{\nu K})/2$  is the corresponding average rotational constant and  $D_{\nu K}$  and  $H_{\nu K}$  are centrifugal distortion constants.  $b_{\nu K} = (B_{\nu K} - C_{\nu K})$ ,  $d_{\nu K}$  and  $h_{\nu K}$  are asymmetry splitting coefficients. The Kronecker  $\delta_{K_i}$  render asymme-

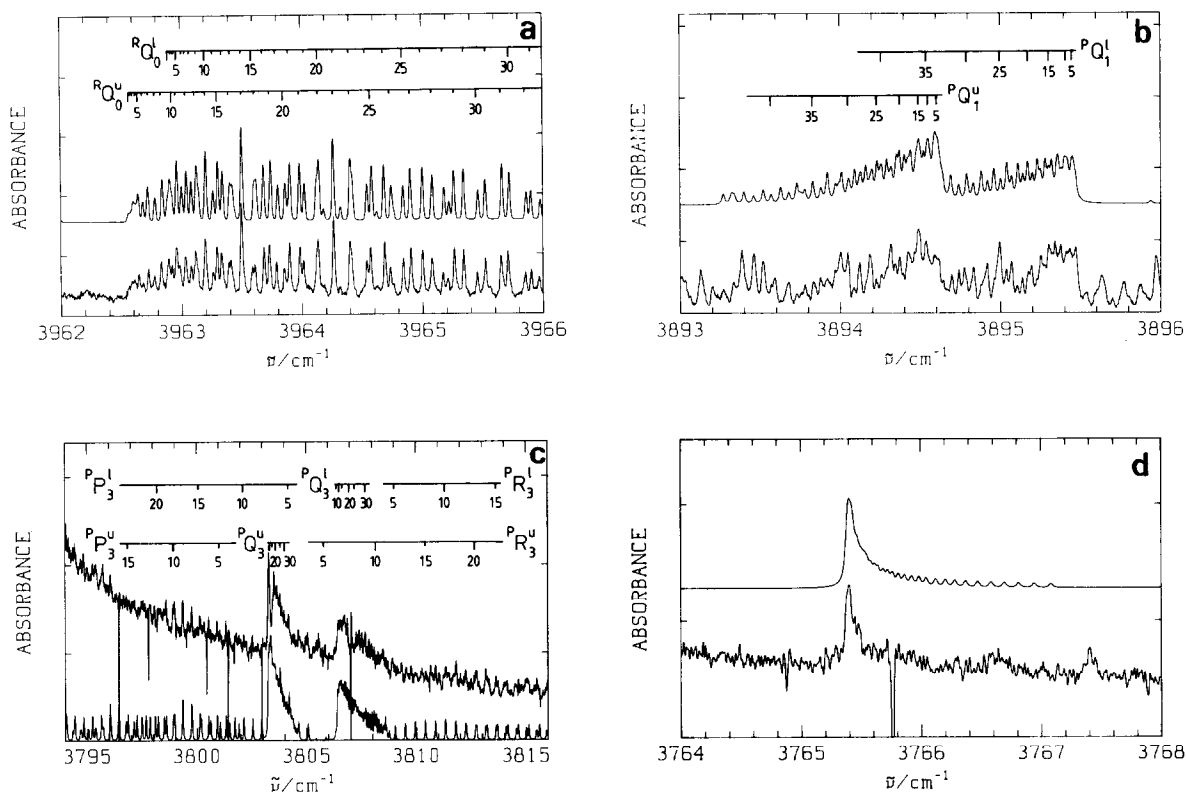


Fig. 7. Q branches of  $\nu_1$  ( $HF$ )<sub>2</sub>: survey of the overall structures showing tunneling splitting (experimental and simulated spectra). (a)  ${}^RQ_0$ , 15 Torr, 251 K, 4 m,  $\Delta\bar{\nu}=0.004$  cm<sup>-1</sup>. (b)  ${}^PQ_1$ , conditions as (a). (c)  ${}^PQ_3$ , 50 mbar, 260 K, 10 m,  $\Delta\bar{\nu}=0.012$  cm<sup>-1</sup>. (d)  ${}^PQ_4$ , conditions as (c).

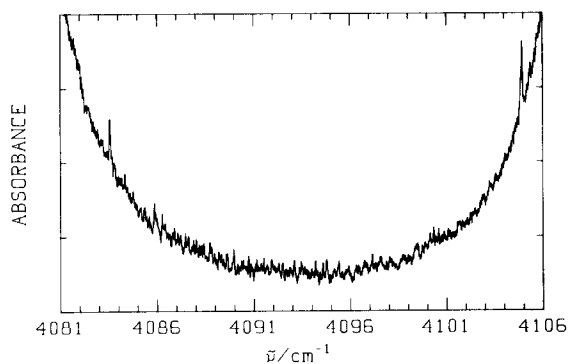


Fig. 8. Spectrum showing peaks due to  ${}^RQ_4$  and  ${}^RQ_5$  in  $\nu_1$  of  $(HF)_2$  (see text, 50 mbar, 260 K, 10 m,  $\Delta\bar{\nu}=0.012$  cm<sup>-1</sup>).

try splittings zero for  $K > 2$ . The upper signs in eq. (3) apply to levels with  $K_a + K_c = J$ , the lower to  $K_a + K_c = J + 1$ . There have been slight variants of this equation in use, which are not too important here. We have also omitted some higher terms in eq. (3) in several fits. Simulations have been shown in fig. 7. They include appropriate line shapes and are generally quite successful with the term formula in eq. (3) or simplifications thereof (see also refs. [28,42–44]). Using the band origins  $\bar{\nu}_{\nu K}$  from these evaluations one obtains the “experimental” term values shown in table 4. They contain the less trivial part of the vibration–rotation–tunneling physics.

In the second approach, one may now try to also describe the  $K$  dependence of term values by a simple term formula. Rigid rotor formulae are clearly inadequate for this purpose. Pine et al. [31] have pro-

Table 4

Summary of term values  $T(\nu, K_a)$  for the ground state and excited stretching states <sup>a)</sup> (in cm<sup>-1</sup>)

$\nu_1$	$\nu_2$	$K_a$	$\Gamma_{\text{tun}} = A^+$	Notes	$\Gamma_{\text{tun}} = B^+$	Notes
0	0	0	0 (504)	a)	0.658690	b)
0	0	1	35.425	b,c)	36.489	b,c)
0	0	2	116.133	c)	118.137	c)
0	0	3	232.63	c)	236.47	c)
0	0	4	(377.13)	d)	386.71	c)
1	0	0	3930.903	e,f)	3931.118	e,f)
1	0	1	3962.867	e,g)	3963.214	e,g)
1	0	2	4038.984	e,h)	4039.69	c,e,h)
1	0	3	4150.71	c,e)	4152.10	c,e,f)
1	0	4	4292.93	c,e)	4296.26	c,e)
			(4300.38)	i)	(4303.11)	i)
1	0	5	(4455.75)	j)	4470 ± 2	e,k)
					(4464)	j)
			(4490.06)	i)	(4495)	i)
1	0	6	(4625)	j)	(4664)	l)
			(4721)	i)	(4642)	j)
0	1	0	3868.079	f,m)	3868.313	f,m)
0	1	1	3900.211	f)	3900.553	f)

<sup>a)</sup> Values in parentheses are estimated or predicted, all other values involve only directly measured wavenumbers and their sums or differences. The anharmonic zero point level has been calculated by quantum Monte Carlo methods using the new analytical potential of ref. [102] and using ab initio points of ref. [51].

<sup>b)</sup> Ref. [28]. <sup>c)</sup> Refs. [42,43].

<sup>d)</sup> Estimated using an ab initio tunneling splitting from ref. [53] and the experimental term value from ref. [42]. Very weak features in <sup>P</sup>Q<sub>4</sub> near 3774, 3771 and 3767.4 cm<sup>-1</sup> would give 377, 380, or 383 cm<sup>-1</sup> for this term value.

<sup>e)</sup> This work. <sup>f)</sup> Ref. [31].

<sup>g)</sup> Ref. [31] gives 3962.866 and 3963.216 cm<sup>-1</sup>, respectively (consistent with our result).

<sup>h)</sup> Ref. [31] gives 4039.122 and 4039.743 cm<sup>-1</sup>, respectively (presumably less accurate than our result, see ref. [42]).

<sup>i)</sup> Estimate using Padé parameters from ref. [31].

<sup>j)</sup> Estimate using Padé parameters from present work (table 5).

<sup>k)</sup> Using an approximate experimental band center for <sup>R</sup>Q<sub>4</sub> at 4083 ± 2 cm<sup>-1</sup>, with error bars arising from uncertainties in *J* assignments.

<sup>l)</sup> Estimate of an approximate band center for <sup>R</sup>Q<sub>5</sub> at 4105 cm<sup>-1</sup> and Padé approximation for the ground state (559 cm<sup>-1</sup>).

<sup>m)</sup> The values are from ref. [31]. Our less accurate data give 3868.078 and 3863.311 cm<sup>-1</sup>.

posed the use of Padé approximants of the following form [86]

$$\tilde{\nu}_{\nu K} = (\tilde{A}_\nu K^2 + \tilde{D}_\nu K^4 + \tilde{H}_\nu K^6 + \dots) \times (1 + \tilde{\alpha}_\nu K^2 + \dots)^{-1}. \quad (4)$$

Table 5 summarizes the constants obtained here from the term values in table 4 for  $\nu=0$  and  $\nu_1=1$  and compares them to the results from a slightly more limited data set used in ref. [31]. One finds substantial changes in the constants, as the data set is increased. This is some indication that the term formula (4), although much better than a rigid rotor term formula, still is of very limited validity. The changes are not due to slight changes in the terms,

which also occur for values of  $K \leq 3$  in the present work. We obtain with these data constants very similar, although not identical, to those of ref. [31], which we do not give here in order to avoid crowding in the table. Essentially, all of the changes arise from adding new terms with  $K=4$ . Table 4 amplifies this point by showing various predictions using the term formula in eq. (4) with different sets of constants. From the results shown in table 4 it is clear that extrapolations using such term formulae remain very uncertain, indeed.

We conclude this section with some observations on hot bands and combination bands. Fig. 9 shows the range of the  $\nu_1$  fundamental from 3969 to 3984 cm<sup>-1</sup>. Compared to the simulation of the cold band

Table 5  
Spectroscopic constants defined in eq. (4) derived from experimental band origins in table 4 (all values in cm<sup>-1</sup>)

Level		Notes	$\tilde{A}$	$\tilde{D}$	$\tilde{\alpha}$	$\tilde{H}$
$\nu$	$\Gamma_{\text{tun}}$					
$\nu=0$	A <sup>+</sup>	a)	41.121892	9.1274596	0.41847146	–
$\nu=0$	B <sup>+</sup>	a)	41.684675	9.5391842	0.42962804	–
		b)	43.003350	15.227814	0.622789	–0.086304
$\nu_1=1$	A <sup>+</sup>	a)	35.942455	7.4653918	0.35806124	–
		b)	37.071122	13.185054	0.56993313	–0.07451941
$\nu_1=1$	B <sup>+</sup>	a)	36.190143	7.8182865	0.37106881	–
		b)	37.095338	12.564842	0.54526069	–0.06333822

a) From ref. [31] using term values to  $K=3$ . b) This work, using term values to  $K=4$ .

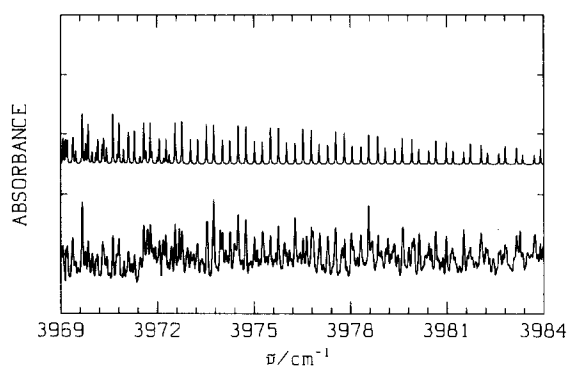


Fig. 9. Simulation of cold band in  $\nu_1$  and experimental spectrum showing lines due to hot band (see text, 50 mbar, 260 K, 10 m,  $\Delta\bar{\nu}=0.012$  cm<sup>-1</sup>).

there are numerous additional lines. From an assignment of about twenty Q- and -R branch lines we could derive an estimate of a band center of  $3971.5 \pm 0.2$  cm<sup>-1</sup>. A fit of intensities suggests that the lower level falls probably in the range 100–200 cm<sup>-1</sup>. One could thus have a hot band with either <sup>R</sup>Q<sub>0</sub> of the hydrogen bond stretching vibration  $\nu_4$  or the tunneling vibration  $\nu_5$ . The anharmonic shift would be +9 cm<sup>-1</sup>, which is consistent with a model invoking strengthening of the hydrogen bond upon excitation of  $\nu_1$  (both with the  $\nu_4$  and the  $\nu_5$  assignment). There remains an open question concerning the second tunneling level, which might be further removed for the  $\nu_5$  assignment. There is a feature near 3975 cm<sup>-1</sup>. A result, which remains independent of any assumptions concerning the assignment is obtained from the line widths: These are found to be pressure broad-

ened (0.04 cm<sup>-1</sup> at resolution 0.012 fwhm), and thus not increased by predissociation broadening beyond this value.

A similar result is also obtained for combination bands near 4270 cm<sup>-1</sup> shown in fig. 10 (measured

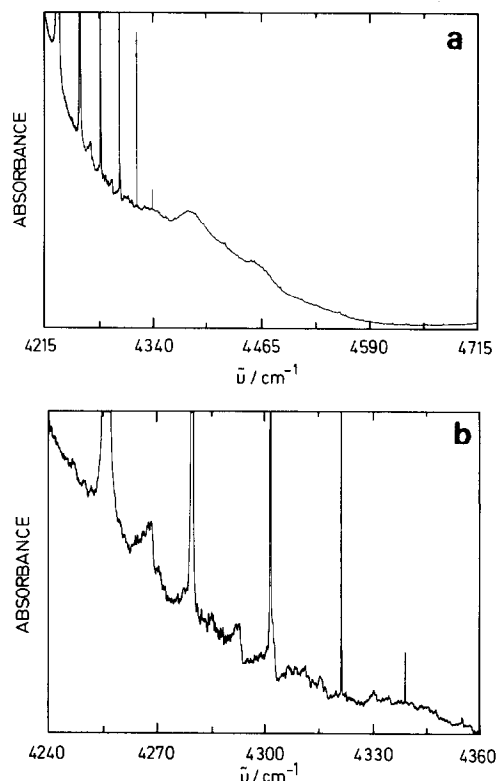


Fig. 10. (a) Combination bands 4215–4715 cm<sup>-1</sup> (375 mbar HF, 298 K, 4 m,  $\Delta\bar{\nu}=0.05$  cm<sup>-1</sup>). (b) Detail of (a).

widths  $0.27 \text{ cm}^{-1}$  at 375 mbar with a resolution of  $0.05 \text{ cm}^{-1}$ , fwhm). Band heads are at  $4268.63$  and  $4293.02 \text{ cm}^{-1}$ , separated by  $338$  and  $362 \text{ cm}^{-1}$  from  ${}^{\text{Q}}\text{Q}_0$  of  $\nu_1$  or by  $400$  and  $425 \text{ cm}^{-1}$  from  ${}^{\text{Q}}\text{Q}_0$  of  $\nu_2$ . The latter intervals are very close to the  $K=1\leftarrow 0$  and  $K=2\leftarrow 1$  transitions of  $\nu_6$  [44]. Also  $\nu_2 + \nu_3$  might be considered. At present the assignment remains open but we shall retain the result of narrow linewidths for later discussion. It is interesting that there is also a broad combination or hot band near  $4390 \text{ cm}^{-1}$ , which looks like a polymer absorption, separated by almost  $900 \text{ cm}^{-1}$  from the main polymer peak.

### 3.3. Rotational fine structure in overtone and combination transitions of the HF stretching vibrations

Fig. 11 shows a survey of the  $N=2$  overtone polyad range including the expected positions of overtones and combinations  $\nu_1=2, \nu_2=2$  ( $\nu_1=1, \nu_2=1$ ). Additional structure between the strong HF monomer absorptions is clearly visible. Comparing to the fundamental range (fig. 6) one might be tempted to assign immediately the peak at  $7746 \text{ cm}^{-1}$  between the P and R branches of the monomer band to  ${}^{\text{R}}\text{Q}_0$  of  $2\nu_1$  and the more complex structures around  $7540 \text{ cm}^{-1}$  to  $2\nu_2$ . The band near  $7647 \text{ cm}^{-1}$  might then even be  $\nu_1 + \nu_2$ . In practice, the situation is much more complex.

Figs. 12 and 13 show relevant parts of spectra of HF/DF mixtures and of DF. From this one can see

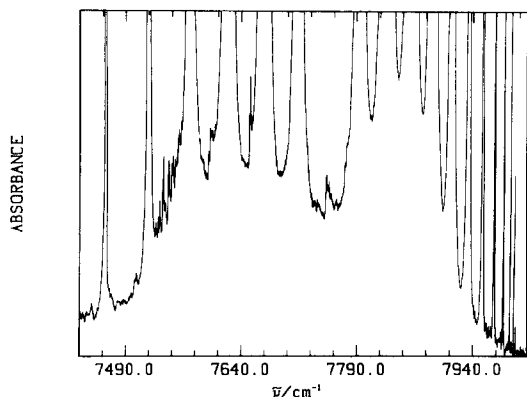


Fig. 11. Survey spectrum of the  $2\nu_1$  and  $2\nu_2$  transitions in  $(\text{HF})_2$  (see text, 370 mbar, 295 K, 4 m,  $\Delta\bar{\nu}=0.1 \text{ cm}^{-1}$ ).

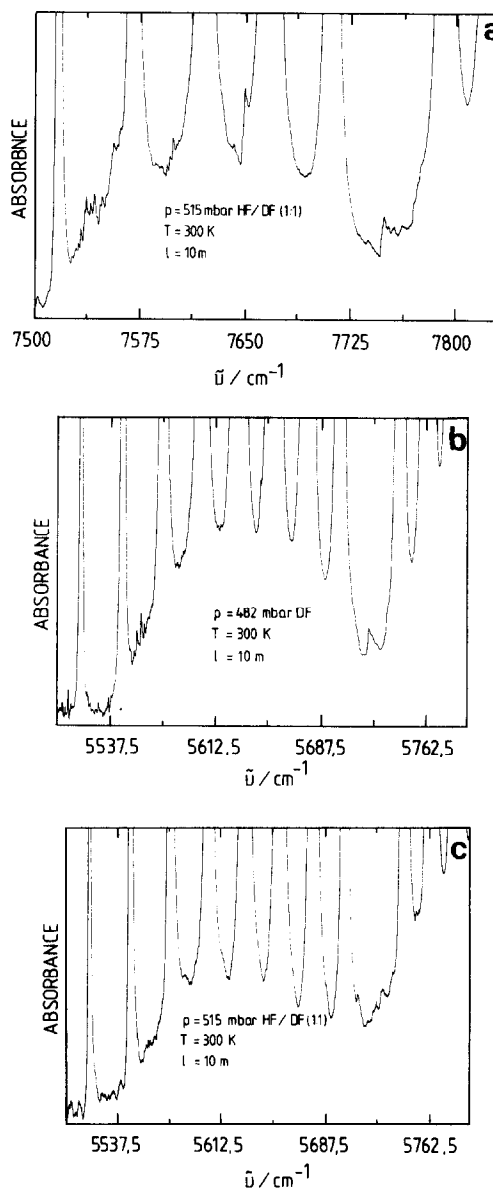


Fig. 12. Survey of the  $2\nu_1$  and  $2\nu_2$  transitions in D-isotopomers of  $(\text{HF})_2$ . (a)  $7500\text{--}7840 \text{ cm}^{-1}$ , 515 mbar HF/DF (1/1), 300 K, 10 m,  $\Delta\bar{\nu}=0.3 \text{ cm}^{-1}$ . (b)  $2\nu_1$  and  $2\nu_2$  of  $(\text{DF})_2$ , the central Q branch being nicely visible between P and R branch of DF monomer (482 mbar, 300 K, 10 m,  $\Delta\bar{\nu}=0.3 \text{ cm}^{-1}$ , absorbance range 0.45–1). (c) HF/DF (1/1) conditions as (a) but range as (b).

that the central band is a general feature, but that there are changes in detail. For  $(\text{DF})_2$  the band is simple and located at  $5722 \text{ cm}^{-1}$ . For  $(\text{HFDF})$  there is an almost unshifted band. Also, for  $(\text{HFDF})$  a doublet

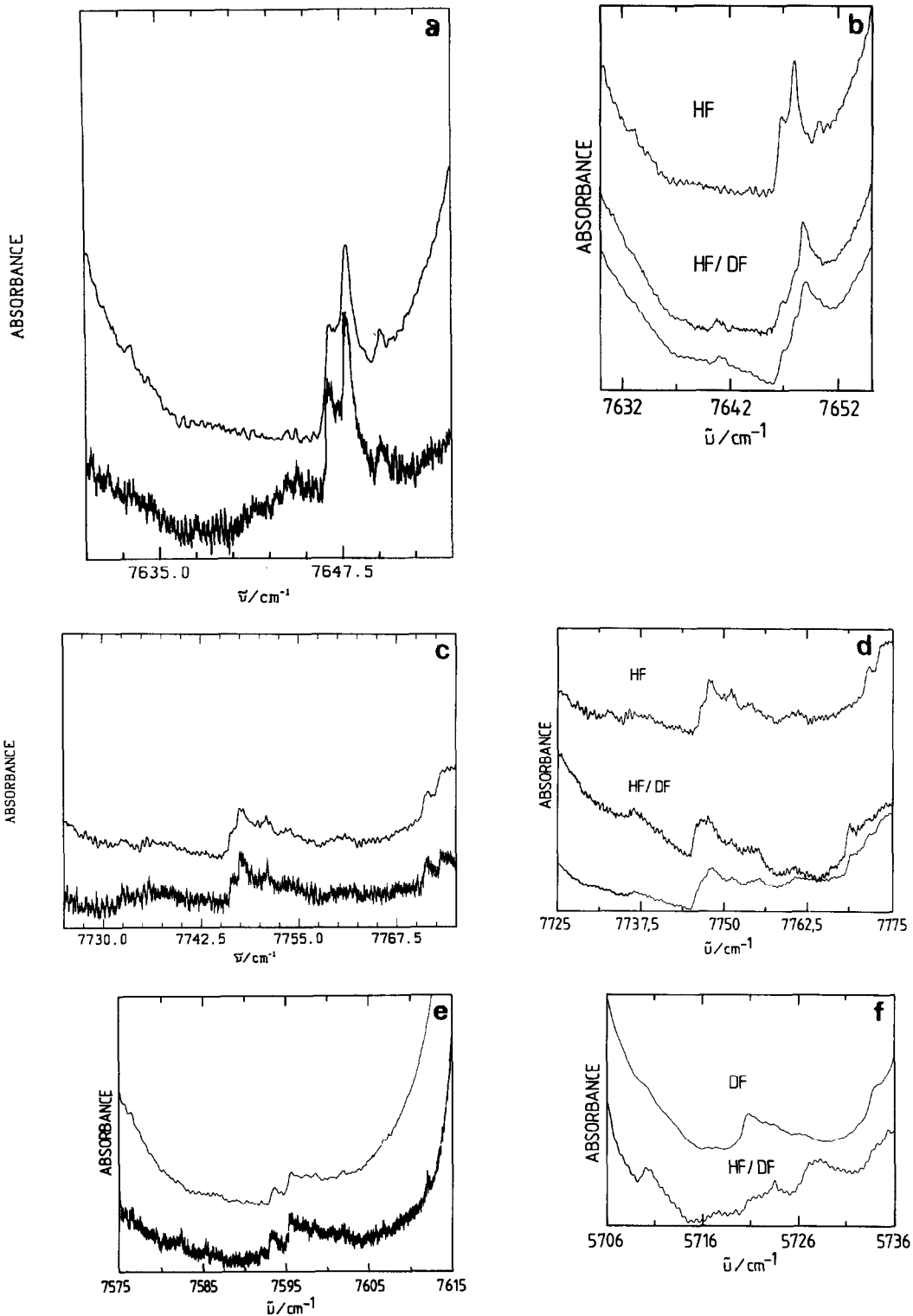


Fig. 13. Details from the spectra in figs. 11 and 12 (see text for detailed discussions). (a)  $(\text{HF})_2$  ( ${}^PQ_2$ , near  $7648\text{ cm}^{-1}$ , see text) 370 mbar, 295 K, 4 m,  $\Delta\bar{\nu}=0.1\text{ cm}^{-1}$  (upper line) and 140 mbar, 265 K, 10 m,  $\Delta\bar{\nu}=0.025\text{ cm}^{-1}$  (lower line). (b) Range as (a) but including HF/DF (1/1) mixtures for the lower lines middle trace: 580 mbar, 300 K, 4 m,  $0.1\text{ cm}^{-1}$ , low trace: 515 mbar, 300 K, 10 m,  $0.3\text{ cm}^{-1}$ . (c)  $(\text{HF})_2$  ( ${}^RQ_0$ ?) conditions as (a). (d) HF/DF mixtures as (b) but range as (c). (e) HF range at  $7600\text{ cm}^{-1}$  (conditions as (a)). (f) Range of  $2\nu_1$ ,  $(\text{DF})_2$  upper trace: 482 mbar DF, lower trace: 515 mbar HF/DF (conditions see fig. 12).

of bands at  $7647 \pm 1 \text{ cm}^{-1}$  seems to be replaced by a single upward shifted peak at  $7648.0 \text{ cm}^{-1}$  (the spectrum shown corresponds to a mixture of isotopomers, of course). A very careful search for a sum transition ( $\nu_1 + \nu_2$ ) in (HFDF) did not reveal any structured absorption. An analysis of the structures must depend at present on these rather limited observations. The doublet structure in (HF)<sub>2</sub> and its disappearance for (HFDF) may be associated with tunneling split bands (cf. fig. 7 for the fundamental). The absence of ( $\nu_1 + \nu_2$ ) in (HFDF) can be either due to very fast predissociation or weakness of the band. We assume the latter, also for (HF)<sub>2</sub>, supported by theoretical estimates of the strength of the combination band. For all other bands in our spectra, the widths are limited by pressure broadening, thus placing a bound to predissociation lifetimes in these overtone absorptions, as discussed in detail below. We were

unable at present to obtain spectra at much lower pressures with rotational line resolution. Therefore  $J$  assignments cannot be used to define the lower states of absorption bands by ground state combination differences. Our analysis will thus rely on assignment of expected Q branches  ${}^P, {}^R Q_K$  of  $2\nu_1$ . Tables 6 and 7 summarize results from two possible assignments of five bands labelled A to E. These bands appear as split Q branches as shown. Because the vibrational symmetry of  $2\nu_1$  is  $A^+$ , the splitting observed in absorption would be the sum of the tunneling splittings in the ground and excited vibrational states. The former are known and thus the latter can be calculated (table 7). Only one difference frequency (B–E) corresponds to a known ground state term difference ( $200 \text{ cm}^{-1}$  between  $K=3$  and  $K=1$ ). This has been used for the assignment I. Unfortunately, band E falls in the range of complex  $\nu_2$  absorption and thus the as-

Table 6  
Q-branch structures assignable to  $2\nu_1$  (all values in  $\text{cm}^{-1}$ )

	A	B	C	D	E
$\tilde{\nu}$	7772.0	7746.8	7647.2	7594.7	7546.5
$\tilde{\nu}_{B^+}$	7771.05	7746.25	7646.58	7593.69	complex
$\tilde{\nu}_{A^+}$	7772.88	7747.35	7647.83	7595.66	complex
assignment I	${}^R Q_2$	${}^R Q_1$	${}^P Q_1$	${}^P Q_2$	${}^P Q_3$
assignment II	${}^R Q_1$	${}^R Q_0$	$({}^P Q_1)?$	?	$(\nu_2)$

Table 7  
 $K$  terms for  $2\nu_1$  with two assignments (all values in  $\text{cm}^{-1}$ )

$K$	Assignment I			Assignment II		
	$\tilde{\nu}$	$\tilde{\nu}_K$	$\Delta\tilde{\nu}_{\text{tun}}$	$\tilde{\nu}$	$\tilde{\nu}_K$	$\Delta\tilde{\nu}_{\text{tun}}$
0	7683.1 <sup>a)</sup>	0 <sup>b)</sup>	(0.19) <sup>c)</sup>	7683.1 <sup>a)</sup> (7717)	0 <sup>b)</sup> 0	0.19 <sup>d)</sup>
1	7711.8	28.6	$\approx 0$	7747.1	63.9 (30)	0.44
2	7782.8	99.6	$\approx 0$	7808.0	124.8 (91)	0.77
3	7889.1	205.9	$\approx 0$ <sup>e)</sup>	–	–	–

<sup>a)</sup> Band maxima were used for these values. Band centers may still be shifted by up to a few  $\text{cm}^{-1}$ .

<sup>b)</sup> The values in columns  $\tilde{\nu}_K$  give the rotational contribution to the term value.

<sup>c)</sup> Consistent with 0, as it is not obtained from band centers but from band maxima.

<sup>d)</sup> If the assignment of 7647 to  ${}^P Q_1$  is omitted and  ${}^R Q_0$  estimated at 7717  $\text{cm}^{-1}$  one obtains the lower terms (in parentheses).

<sup>e)</sup> From the peak splitting one has formally  $-0.2 \text{ cm}^{-1}$  (see footnote c).

signment is uncertain. Nevertheless, all other bands find a straightforward assignment with I. <sup>R</sup>Q<sub>0</sub> is missing, as it is predicted to fall at the position of the strong monomer line at 7710 cm<sup>-1</sup>. The prominent peak at 7746 cm<sup>-1</sup> would be <sup>R</sup>Q<sub>1</sub> and the band center near 7680 cm<sup>-1</sup>. The sequence of *K* levels would be consistent with a further tightening up of the (HF)<sub>2</sub> structure (smaller effective *A* constant) and otherwise similar in pattern to the ground and first excited state. A surprising consequence is an essentially zero tunneling splitting for all *K* levels in 2ν<sub>1</sub>. This seems somewhat unlikely, although not impossible (0.19 for *K*=0 is not inconsistent with "0" at this level, noting that the band centers have not been obtained by a rotational analysis and that even slightly negative values for the splittings occur).

The second assignment II is attractive by analogy of <sup>R</sup>Q<sub>0</sub> with the fundamental transition. However, all the other subbands have a difficult assignment. From <sup>R</sup>Q<sub>0</sub> one would predict <sup>P</sup>Q<sub>2</sub> at 7630 cm<sup>-1</sup>, where there is weak, by no means convincing structure. On the other hand, the strong band at 7647 cm<sup>-1</sup> could be assigned to <sup>P</sup>Q<sub>1</sub>, leading to a most unusual pattern for the *K* levels (table 7). Such a pattern would imply a shift of the levels *K*=1, ν<sub>1</sub>=2 and perhaps *K*=0, ν<sub>1</sub>=2 by some interaction with another level. The band center would still be near 7680 cm<sup>-1</sup>. Otherwise one might leave bands C and D unassigned (they cer-

tainly belong to (HF)<sub>2</sub>, though), and estimate a band center at 7717 cm<sup>-1</sup>. A compromise estimate for the band origin of ν<sub>1</sub> would be 7700 ± 20 cm<sup>-1</sup>. The shift with respect to the HF monomer would be 50 ± 17 cm<sup>-1</sup>. Theoretical estimates by Liu and Dykstra [87] give 65 cm<sup>-1</sup> for the shift and a local mode model calculation for ν<sub>1</sub> on the potential surface of refs. [52,53,102] also predicts rather low wavenumbers for 2ν<sub>1</sub>, in agreement with assignment I (shift of 71 cm<sup>-1</sup>). The tunneling splittings will be discussed below in more detail. If band C were assigned as <sup>R</sup>Q<sub>0</sub>, one would predict 2ν<sub>1</sub> at 7620 cm<sup>-1</sup>, which seems low.

The situation for 2ν<sub>2</sub> is even more complex than for 2ν<sub>1</sub>. Fig. 14 shows details of spectra for (HF)<sub>2</sub>, HF/DF and (DF)<sub>2</sub>. There is no doubt that the sharp structures are to be associated with the dimer, as estimated from the partial pressure and temperature dependence and by comparison with the well understood fundamental. The detailed assignment is difficult. Fig. 14b shows that doublet structures for (HF)<sub>2</sub> become simple for HF/DF, suggesting again the interpretation as tunneling doublets. As discussed, some of the structure may be assigned to <sup>R</sup>Q<sub>*K*</sub> branches of 2ν<sub>1</sub>. One would expect that <sup>Q</sup>Q<sub>0</sub> and <sup>Q</sup>Q<sub>1</sub> of 2ν<sub>2</sub> are separated by more than 3.2 cm<sup>-1</sup> (the value in the fundamental). Observed separations of 7 and 4 cm<sup>-1</sup> in fig. 14a correspond presumably to band

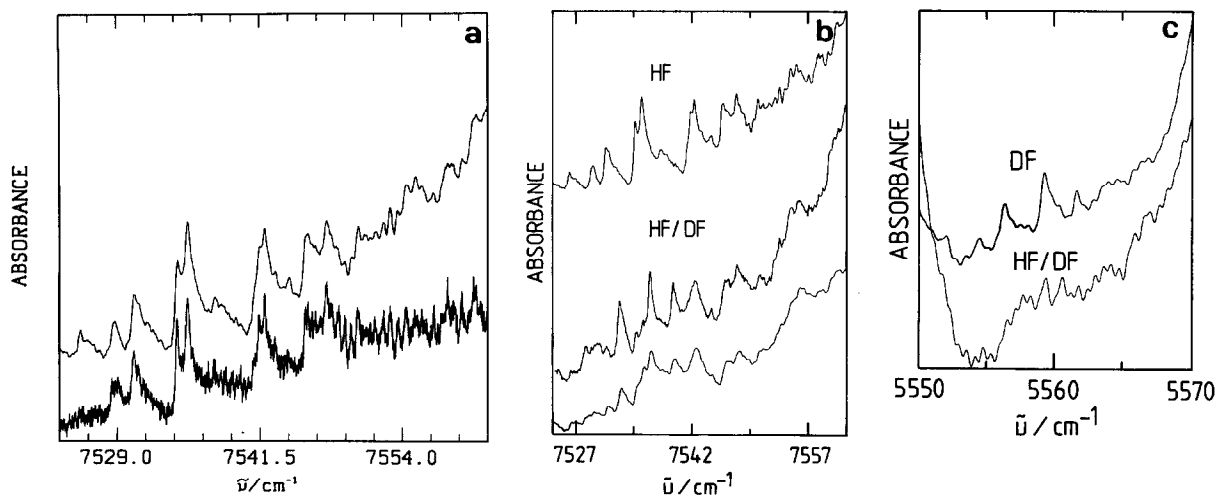


Fig. 14. Details of 2ν<sub>2</sub> (2ν<sub>1</sub>?) of (HF)<sub>2</sub> and isotopomer spectra. (a) (HF)<sub>2</sub> conditions see fig. 13a (from ref. [45]). (b) (HF/DF) mixture conditions as fig. 13b. (c) (DF)<sub>2</sub> (upper trace) and mixture of HF/DF (lower trace), conditions see fig. 12.

heads in the P branch (already weakly visible in the fundamental), due to the tightening of the hydrogen bond with vibrational excitation. Assuming that a “typical” head is at 7542, separated by about 15 cm<sup>-1</sup> from the center, the latter is estimated to be 7557 ± 15 cm<sup>-1</sup>. This is consistent with theoretical estimates (7562 cm<sup>-1</sup>, with a 189 cm<sup>-1</sup> shift from the monomer [87] or about 7550 cm<sup>-1</sup> with a local mode model on the potential of refs. [52,53,102]). Our previous estimate of 7542 cm<sup>-1</sup> is probably a low estimate for the band center of  $\nu_2$  [45]. If one is willing to accept an interpretation of the splitting of about 0.5 cm<sup>-1</sup> in the head at 7542 as a  $^{\infty}Q_0$  splitting and of about 0.9 cm<sup>-1</sup> in the band at 7535 cm<sup>-1</sup> as a  $^{\infty}Q_1$  splitting, this would be consistent with a negligible tunneling splitting in the vibrationally excited state and a shift of  $^{\infty}Q_1$  to low wavenumbers by 7 cm<sup>-1</sup>, linear with  $\nu_2$  compared to the fundamental.

A firm result from these spectra is consistently an observation of sharp, essentially pressure limited line structure ( $\Delta\bar{\nu}(\text{fwhm}) \approx 0.1$  to 0.16 cm<sup>-1</sup>) for all isotopomers and observed bands. For (HF)<sub>2</sub> the pressure broadening coefficient was determined to be about 13 cm<sup>-1</sup>/MPa and experimental pressures were around 10 kPa. This provides a bound on the lifetimes for predissociation  $\gtrsim 50$  ps. Spectra at much lower pressures or using quite different techniques would be needed to improve upon this analysis. Nevertheless, the present observations provide a first step also towards such experiments in defining spectral regions where sharp structure can be observed.

This result is amplified (with even larger pressure broadening) by the observation of line structure for (HF)<sub>2</sub> also in the  $N=3$  and  $N=4$  polyads (i.e.  $N=\nu_1+\nu_2=3$  and 4). Examples of spectra are shown in fig. 15. Pressure dependence, temperature dependence and isotopic variants all demonstrate that the observed line-like structures belong to (HF)<sub>2</sub>. Although the structure not belonging to the monomer in fig. 15c is hardly above the noise level, it is reproducible and was shown not to arise from artifacts (say, from the wings in the strong monomer lines and apodization). An analysis of the structures was not even attempted, but the line widths provide again bounds for predissociation lifetimes. For the higher overtones our study is clearly exploratory and more work on these is needed. The  $N=4$  region is easily accessible to laser spectroscopy, such as ICLAS [88] or perhaps photoacoustic spectroscopy [89].

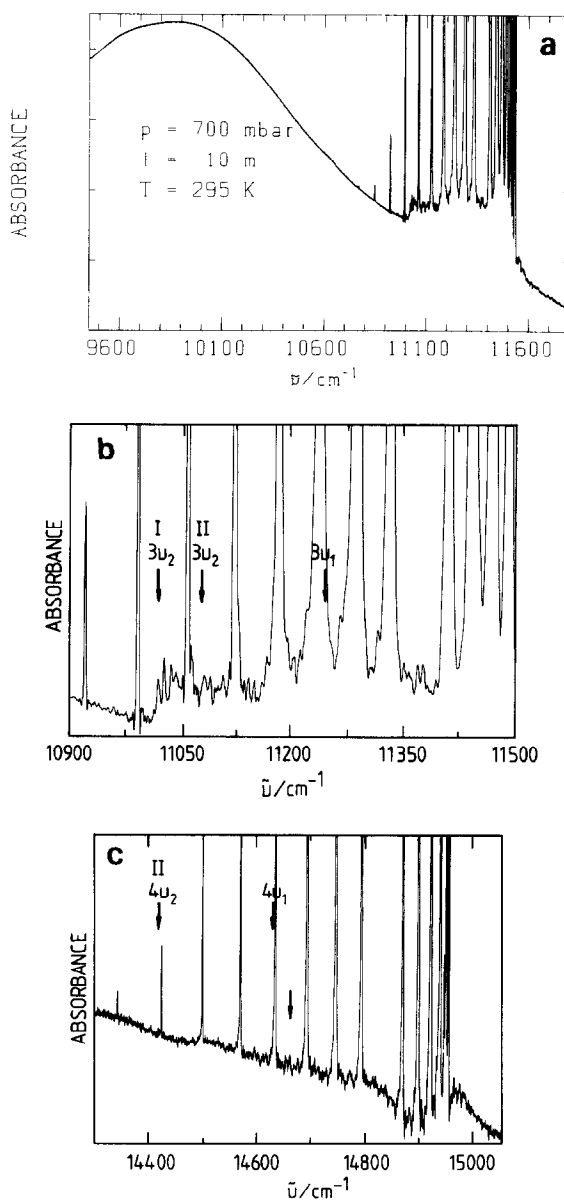


Fig. 15. Higher overtones of the HF stretching vibrations in (HF)<sub>2</sub>. (a) Survey of the  $N=3$  polyad region including polymer absorption in (HF)<sub>n</sub> 700 mbar HF, 295 K, 10 m,  $\Delta\bar{\nu}=0.7$  cm<sup>-1</sup> (from ref. [46]). (b) Detail of (a) absorbance range 0.056–0.13. (c)  $N=4$  polyad range (680 mbar, 300 K, 10 m,  $\Delta\bar{\nu}=0.7$  cm<sup>-1</sup>, absorbance range 0.02–0.12).

#### 4. Discussion

We shall provide in this section a discussion and

summary of the main results on how rearrangement tunneling and predissociation in (HF)<sub>2</sub> depends upon the excitation of various modes. We will use the conceptual framework of vibrationally adiabatic separation of the low-frequency modes from high-frequency modes, which has been found useful in intramolecular vibrational redistribution and spectroscopy [90–94] and unimolecular reaction kinetics (e.g. adiabatic channel model [6,8,95]). A quantitative theory is not attempted, at present.

#### 4.1. Mode selective tunneling splittings for rearrangement of the hydrogen bond

Table 8 summarizes the known and estimated tunneling splittings for (HF)<sub>2</sub> as a function of the excitation of various modes: the tunneling mode  $\nu_5$ , the out of plane bending mode  $\nu_6$ , the  $K_a$  rotational motion and the high-frequency stretching modes  $\nu_1$  and  $\nu_2$ . Not surprisingly, rearrangement tunneling is promoted strongly by excitation of the tunneling mode  $\nu_5$ . There is, however, also some enhancement of rearrangement when exciting the  $\nu_6$  mode (out of plane bending at 400 cm<sup>-1</sup>, close to the effective barrier for the tunneling motion). Also when exciting  $K_a$  rotation tunneling is promoted (by a factor of more than five when putting  $\approx 200$  cm<sup>-1</sup> into this motion). With respect to energy efficiency  $K_a$  rotation is thus second to  $\nu_5$ . This can be understood, if one notes that this rotational motion pushes the off axis H atom in the same direction as the tunneling mode  $\nu_5$ . Also,

excitation of  $\nu_6$  loosens the hydrogen bond on the average and thus facilitates tunneling. Nevertheless, rearrangement with excitation in these modes is still slow and follows a rather regular pattern, almost by simple combination of contributions, when comparing, for instance,  $K=1$  and  $K=2$  for  $\nu=0$  and  $\nu_6=1$ . One may thus consider even these modes as adiabatically decoupled, with a modest change of the effective tunneling potential when exciting  $K_a$  or  $\nu_6$ . The situation is even more striking for the stretching fundamentals and overtones ( $\nu_1$  and  $\nu_2$  excitation). Here one finds a decrease of the effective tunneling rates with vibrational excitation, as noted before [31–33]. Our overtone results confirm this trend particularly for the more likely assignment I of section 3.3. In an adiabatic picture this corresponds to an increase of the effective barrier for the tunneling mode from about 300 cm<sup>-1</sup> in  $\nu=0$  to about 400 cm<sup>-1</sup> in  $\nu_1=1$  [31]. The situation is complicated, because for (HF)<sub>2</sub> one has two close lying vibrationally adiabatic potentials for the fundamental range  $N=1$  ( $\nu_1=1$  and  $\nu_2=1$ ) and three for  $N=2$  ( $\nu_1=2$ ,  $\nu_2=2$ ,  $\nu_1=\nu_2=1$ ). Fraser [96] has recently discussed this situation in detail, favouring a mechanistic picture, where the decrease of tunneling rates with  $\nu_1$  or  $\nu_2=1$  results from the difficulty in exchanging quanta between the two modes. Unfortunately, Fraser did not predict tunneling splittings for  $\nu_1=2$ . Another test for his assumption might be provided, if the combination tone  $\nu_1=\nu_2=1$  is analyzed, which was not yet possible. (The “vibrational exchange argument” will not hold

Table 8  
(HF)<sub>2</sub> tunneling splittings as a function of excitation of various modes and their combination with  $K_a$  rotation

	$\Delta\bar{\nu}$ (GHz)					Notes
	$K=0$	$K=1$	$K=2$	$K=3$	$K=4$	
ground state	19.7470	31.9110	60.074	115	–	a)
$\nu_5=1$	424	749	1259	1910	2613	b)
$\nu_6=1$	–	48.77	103.25	–	–	c)
$\nu_1=1$	6.5	10.49	21.1	41.1	100	d)
$\nu_2=1$	7.0	10.2	–	–	–	e)
$\nu_1=2$	<6	<6	<6	<6	–	f)
	$\approx 5.6?$	$\approx 13$	$\approx 23$	–	–	g)

a) Experiment see refs. [24,28,31,42]. b) Theory [52,53]. c) Experiment [43,44].

d) Refs. [31,42] and this work. e) Ref. [31], also this work for  $K=0$ .

f) This work, with assignment I, section 3.3, still uncertain estimate.

g) This work, with assignment II, section 3.3, less likely estimate.

here.) We still would think that an interpretation based on a change of effective adiabatic potential may be quite adequate [42]. Such an interpretation provides the right trends for the increase of barrier from  $v=0$  to  $v_1=1$  and  $v_1=2$  just by zero-point energy arguments (particularly with assignment I) and a strong decrease of tunneling splittings in  $v_1=2$ . Further indirect evidence for a change of effective potentials comes from our measured shift of  $+9\text{ cm}^{-1}$  for the hot band of  $v_1$  with a low-frequency mode (which is perhaps the tunneling mode  $\nu_5$ , see section 3.2) and from the isotope effect on the barrier [31]. The interpretation in terms of a change of effective potentials is also consistent with a tightening up of the structure of the dimer as seen in the effective rotational constants of  $\nu_1$ ,  $\nu_2$  and  $2\nu_1$  (again assignment I, consistently). A prediction from this interpretation would be an increased effective dissociation energy in  $v_1=1$  or  $2$  ( $\nu_2=1$  or  $2$ ), as discussed in more detail below. We note that our discussion is in perfect agreement with the qualitative ideas put forward originally by Stepanov [4]. One might be tempted to think that in this picture there should be a great difference for the modes  $\nu_1$  (ineffective) and  $\nu_2$  (bound HF, very effective in changing the potentials). For symmetry reasons, however, the situation is not quite as simple and one must treat all the various potentials in the  $N=v_1+v_2$  polyads. The effective adiabatic potentials are coupled by a number of terms including Darling–Dennison and related resonances in the overtones.

Whatever the detailed dynamical interpretation of the tunneling splittings may be, the very substantial mode selectivity shown by the results in table 8 has important implications for any discussion of hydrogen bridge rearrangement processes in the  $(\text{HF})_2$  molecule and perhaps even in hydrogen bonded liquids in general. Of particular interest would be a further systematic study of the other isotopomers in this context.

#### 4.2. Predissociation rates and comparison with RRKM theory or quasi-equilibrium theories of unimolecular reactions

The unimolecular dissociation of  $(\text{HF})_2$  has many aspects of a prototype vibrational predissociation of hydrogen bound molecules. It can be readily dis-

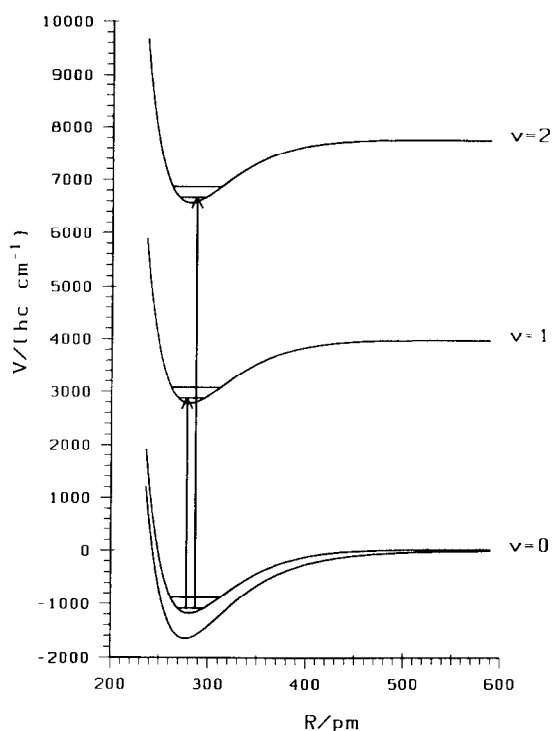


Fig. 16. Electronic potential (lowest function) and several adiabatic channels (upper functions) as a function of the center of mass distance  $R$  of the monomer units in  $(\text{HF})_2$  (see detailed discussion in the text).

cussed in terms of vibrationally adiabatic channel potentials and resonance scattering theory [6]. Fig. 16 shows a semi-quantitative drawing of some adiabatic channels relevant for the fundamental and overtone absorptions. The lowest function shows the pure electronic potential. The next potential is the lowest adiabatic channel, calculated approximately, following the procedure of ref. [95] with an interpolation parameter  $\alpha=1\text{ \AA}^{-1}$ . This effective potential supports bound states, the lowest one shown being the vibrational ground state. The energy zero of both the lowest channel and the electronic potential was taken at  $v=0$  for visualization, in reality they differ by the zero-point energy of  $2\text{HF}$ . The next two channels shown are the adiabatic channels with  $v_1=1$  and  $v_1=2$ . Of course, there are many further adiabatic channels, which are not shown. Only few of them are dynamically similar to the ones shown:  $\nu_2=1$  and  $\nu_2=2$ , as well as  $\nu_1=\nu_2=1$ , which have been omitted.

The particularities of (HF)<sub>2</sub> dissociation can be discussed in the following framework. The four low-frequency modes and rotation generate a background rovibrational density of states  $\rho'(E, J)$ . One might assume that statistical or quasi-equilibrium theories may perhaps hold for these, in the framework of the adiabatic channel model for the rate constant [6]:

$$k(E, J) \approx \frac{W'(E, J)}{h\rho'(E, J)}, \quad (5)$$

where  $W'(E, J)$  is the number of open adiabatic channels of the low-frequency modes at energy  $E$  and angular momentum  $J$  ( $M$ , parity etc.). Below the high-frequency channels  $\nu=1$  and  $\nu=2$  shown one has

$$W'(E, J) \approx W(E, J) \quad (6a)$$

and

$$\rho'(E, J) \approx \rho(E, J). \quad (6b)$$

Here  $\rho(E, J)$  and  $W(E, J)$  are the total density and number of open channels. The first question to be answered by the experiments concerns the validity of quasi-equilibrium statistical theories for the particular, isolated levels seen in the spectra (as discussed below, this is to some extent contrary to the intentions of general statistical theory, but the question is of interest anyway). Generally, one would have to calculate the adiabatic channels and  $W(E, J)$  on a given potential for the dissociation of (HF)<sub>2</sub>, the result depending heavily upon the potential. In practice, one can derive a simple estimate and a rigorous bound to the statistical  $k(E, J=0)$  by a simple vibrational RRKM or RRK estimate:

$$k(E)_{\text{RRKM}} = \frac{W^*(E^*)}{h\rho_{\text{vib}}(E)}. \quad (7)$$

Here  $\rho_{\text{vib}}(E)$  is the vibrational density of states, and  $W^*(E^*)$  the number of levels of the transition state with available energy  $E^*$ . In the classical RRK limit for a tight transition state one has with the number of vibrational degrees of freedom,  $S$ :

$$k(E)_{\text{RRK}} = \left(\frac{E^*}{E}\right)^{S-1} \nu_{\text{RK}} = \left(\frac{E-E_0}{E}\right)^{S-1} \nu_{\text{RK}}. \quad (8)$$

We use the frequency  $\nu_{\text{RK}}$  of the reaction coordinate (the F...H-F stretching mode) and  $E_0$  the threshold energy, for the simple bond fission equal to  $\Delta H_0^\ddagger$ .

Now  $k(E)_{\text{RRK}}$  is an absolute low estimate of  $k(E)_{\text{RRKM}}$  with tight or semitight transition states. The latter may use scaling factors  $n \approx 0.7$  for the frequencies in the transition state:

$$\nu^* = \nu_0 - n(\nu_0 - \nu_{\text{final}}). \quad (9)$$

Furthermore,  $k(E)_{\text{RRKM}}^{\text{tight}}$  provides a very low estimate of the correct statistical  $k(E, J=0)$ , eq. (5). Table 9 summarizes statistical rate constant estimates using these low bounds and some experimental results. It is evident that the measured "rate constants" obtained from experimental predissociation widths  $\Gamma_p$  or bounds thereof ( $\Gamma_{\text{measured}} \geq \Gamma_p$ ) by

$$k_{\text{exp}} = 2\pi\Gamma(\text{fwhm})/h, \quad (10a)$$

$$k_p \leq k_{\text{exp}}, \quad (10b)$$

in all cases are much smaller than the lowest estimate from statistical theory. This clearly disproves the validity of RRKM theory for these isolated (HF)<sub>2</sub> resonances.

In the appreciation of this result one must note that the general statistical theory for statistical scattering lifetimes provides only an inequality for the average dissociation rate constant of scattering resonances (density  $\rho(E, J)$ ), namely [6],

$$\langle k_{\text{true}}(E, J, \dots) \rangle_{\Delta E} \leq \frac{W(E, J, \dots)}{h\rho(E, J, \dots)}. \quad (11)$$

According to the discussion in refs. [6,97], in principle large deviations for individual resonances are possible. Therefore the long lifetimes of (HF)<sub>2</sub> resonances could be explained either as indicating a reduction of the average rate constant following eq. (11) or as a large, statistically insignificant fluctuation from the average for the specific resonances observed in the spectra, or both. All these possibilities could be incorporated in a more general statistical theory [10]. The last two possibilities are most likely and in this context we plan to also measure the thermal rate constant for reaction (2), which will provide evidence on the average rate constant at modest energy. In any case, ordinary RRKM or quasiequilibrium theory (eq. (7)) fails for the observed rates. It also fails to predict the clearly mode selective increase of dissociation rate upon excitation of  $\nu_2$ , observed in the fundamental (table 9). Our results on the overtones at present show too much pressure

Table 9  
Rate constants for the unimolecular dissociation of (HF)<sub>2</sub>

Level <sup>a)</sup> (term) (cm <sup>-1</sup> )	$k / (10^{12} \text{ s}^{-1})$				Notes
	$k_{\text{exp}}^{\text{b)}}$	$k_{\text{RRKM}}^{\text{semitight}}$	$k_{\text{RRKM}}^{\text{tight}}$	$k_{\text{RRK}}$	
(3850)		24	0.9	0.5	c)
$\nu_1, K=0, A^+$	$4.0 \times 10^{-5}$				d)
$\nu_1, K=0, B^+$	$6.0 \times 10^{-5}$				d)
$\nu_1, K=1, A^+$	$6.4 \times 10^{-5}$				d)
$\nu_1, K=1, B^+$	$7.4 \times 10^{-5}$				d)
$\nu_2, K=0, A^+, B^+$	0.002				d)
(7600)		67	2.2	1.5	c)
$2\nu_1, 2\nu_2$	0.02				c)
(11100)		105	3.3	2.2	c)
$3\nu_1, 3\nu_2$	0.2				c)
(14350)		139	4.2	2.6	c)
$4\nu_1, 4\nu_2$	1				c)

<sup>a)</sup> The term value for the calculation is a low estimate for the average experimental level (in cm<sup>-1</sup>). One has  $k(E)_{\text{RRKM}} \geq k(E_{\text{low}})_{\text{RRKM}}$ .

<sup>b)</sup>  $k_{\text{exp}} = 2\pi c \tilde{\Gamma}$  is calculated from the experimental linewidth  $\tilde{\Gamma}$  (fwhm, in cm<sup>-1</sup>) as measured. This provides a rigorous bound for predissociation  $k_p \leq k_{\text{exp}}$ . For the pressure broadened overtones the inequality holds in any case.

<sup>c)</sup> Results from this work, "semitight" transition state with  $n=0.7$  in eq. (9), with a somewhat arbitrary set of frequencies, different from table 3.  $k_{\text{RRK}}$  has been recalculated with the most recent data [102], the differences being not important.

<sup>d)</sup> Results from ref. [33], generally consistent with previous work [30,31,37-39].

broadening to confirm this trend. Also our measurement of the isotope effect on linewidth in (DF)<sub>2</sub> overtone spectra provides bounds with very similar conclusions as for (HF)<sub>2</sub> and is thus not reproduced in detail, here (see the figures of spectra, which were taken at slightly reduced resolution).

The failure of RRKM theory obviously raises the question of alternative treatments. In a simplified discussion of resonance scattering eq. (5) is just one limiting case of resonance lifetimes contained in the general model of Mies and Krauss [95,99]

$$k_c(E, J) = \left( \sum_a \gamma_{ac}(E, J) \right) / h\rho(E, J), \quad (12a)$$

$$\gamma_{ac} = 2\pi \Gamma_{ac} \rho_a / (1 + \frac{1}{2} \pi \Gamma_{ac} \rho_a)^2, \quad (12b)$$

$$\Gamma_{ac} = 2\pi |V_{ac}|^2 \rho_a. \quad (12c)$$

The sum is extended over the dissociation channels  $a$ . The formal coupling width  $\Gamma_{ac}$  is calculated with the average (or constant) square coupling  $|V_{ac}|^2$  of the coupled resonance state  $c$  to the continuum  $a$ , with density of states  $\rho_a$ . Eq. (5) results from (12a) by

replacing the formal transmission coefficient by its maximum value ( $0 \leq \gamma_{ac} \leq 1$ ). In the limiting case of very weak coupling  $\Gamma_{ac}$  one obtains the usual perturbative golden rule formula for the decay of an isolated resonance into separate continua (channels)  $a$ :

$$k_{c,\text{pert}} = \frac{2\pi}{h} \sum_a 2\pi |V_{ac}|^2 \rho_a. \quad (13)$$

Even if this limit is satisfied, the calculated result clearly depends upon the dynamical model used to calculate the coupling  $V_{ac}$ . Very different predictions have thus resulted for predissociation lifetimes. These include very low early estimates with  $k \approx 5 \times 10^{-3} \text{ s}^{-1}$  for  $\nu_1$  and  $5 \times 10^{-2} \text{ s}^{-1}$  for  $\nu_2$  (see ref. [67] but also the more recent references. [69,70]) and simplified coupled channel calculations with the artificial channel method giving about  $6 \times 10^8 \text{ s}^{-1}$  for  $\nu_2$  and  $1.1 \times 10^9 \text{ s}^{-1}$  for  $2\nu_2$ , roughly consistent with experiment [72,73].

The observed low dissociation rates are consistent with a description of the (HF)<sub>2</sub>-HF-stretching vibrational predissociation in terms of an adiabatic

separation similar to predissociation on electronically excited adiabatic states. In the theory of radiationless transitions [98] two limiting cases may be distinguished. The first case (i) would be direct predissociation from an excited state in the upper potentials of fig. 16 to the continuum. The second (ii) has first transfer of excitation from the high-frequency modes to the low-frequency modes of the dimer (intramolecular vibrational redistribution similar to "internal conversion" in the electronic case, transition from an upper potential in fig. 16 to a lower one). In this case the observed linewidths might be redistribution limited and the unimolecular dissociation might be still much slower (cf. inequality (10b)). If the dissociation after redistribution can be described by statistical theory, this latter possibility would not be realized, however. Thirdly (iii) there is an intermediate case with stepwise predissociation mediated by far off resonant states of low-frequency modes. This last case is similar to (ii) but with a low density of intermediate levels from low-frequency modes.

Fig. 17 shows some estimated densities of states that allow us to obtain some conclusions concerning the possible predissociation mechanisms. These densities have been calculated using harmonic and Morse oscillators and including the  $K$  rotor by direct count [100,95]. The tunneling splitting has been neglected and in order to include parity conservation one would have to divide the results in the figure by 2 [101]. In the region of the fundamentals  $\nu_1$  and  $\nu_2$  the total density of states  $\rho(E, J)$  is less than about 100 states per  $\text{cm}^{-1}$  and thus the separation of states is large compared to the width of resonances. Except for unusual "structured" densities this excludes mechanism (ii) of predissociation but leaves (i) and (iii) possible. In the regions of the higher overtones the density of levels rises but for  $J=0$  it is hardly ever high enough to allow for a change to mechanism (ii) with a second statistical step satisfying the condition [97]

$$\Gamma \approx \Delta E \gg \rho(E, J)^{-1}. \quad (14)$$

For larger  $J$  and with pressure broadening conditions a change of mechanism might be more easily possible. These estimates show also that measured linewidths in the fundamental and probably the first overtones will correspond to predissociation and not

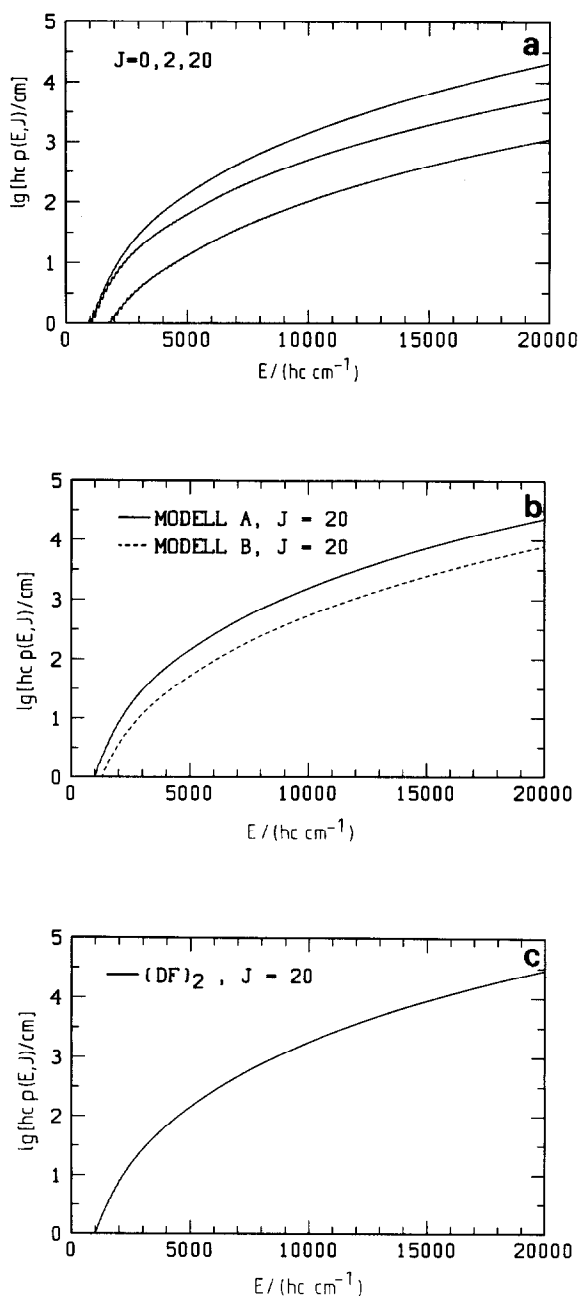


Fig. 17. Densities of states  $\rho(E, J)$  of  $(HF)_2$  and  $(DF)_2$  estimated by direct count with simple rovibrational models. (a) Rotational dependence  $J=0$  lower,  $J=2$  middle,  $J=20$  upper function in  $(HF)_2$ . (b) Model dependence with two different sets of fundamentals estimated within current uncertainties, particularly at high energies there are further uncertainties from nonrigidity. (c)  $(DF)_2, J=20$ .

to intramolecular redistribution under isolated molecule conditions.

The present discussion also readily explains why there is still sharp line structure in the hot band and combination transitions of  $\nu_1$  or  $\nu_2$  observed in section 3.2. The energy of the corresponding excited states is below the dissociation limit of the upper effective potential and thus the predissociation remains slow, similar (not necessarily identical) to  $\nu_1$  or  $\nu_2$ , following essentially the same mechanism.

### 4.3. The adiabatic and crude adiabatic picture of rearrangement tunneling and predissociation

The spectroscopic results and the related kinetic processes of rearrangement and predissociation can be understood in terms of two concepts, which are related but not identical, (i) the crude adiabatic and (ii) the adiabatic separation of high-frequency from low-frequency modes.

(i) In the crude adiabatic picture each HF unit I or II is characterized by its stretching quantum state  $\nu_I$  or  $\nu_{II}$  with associated average HF bond distances  $r_{vI}$  and  $r_{vII}$ . Taking these to be constant one obtains an effective potential in the remaining four internal degrees of freedom ( $q_3, q_4, q_5, q_6$  as generalized coordinates)

$$V(r_1, r_2, q_3, q_4, q_5, q_6) = V(r_{vI}, r_{vII}, q_3, q_4, q_5, q_6). \quad (15)$$

The dynamical problem for the four low-frequency modes is thus four dimensional with fixed values of  $r_{vI}$  and  $r_{vII}$  given  $\nu_I$  and  $\nu_{II}$  and could be taken directly from an electronic potential function without further dynamical calculation.

(ii) In the adiabatic picture one introduces in addition an implicit dependence of  $r_{vI}$  and  $r_{vII}$  and the corresponding energies as a function of the coordinates  $q_3, q_4, q_5, q_6$  in terms of the following approximation scheme for the Hamiltonian and wavefunction

$$\hat{H} = \hat{H}_0 + \hat{H}_1, \quad (16)$$

$$\hat{H}_0 \Psi_{nm}^0 = E_{nm}^0 \Psi_{nm}^0, \quad (17)$$

$$\Psi_{nm}^0 = \phi_n(q, r) \xi_{nm}(q). \quad (18)$$

The  $q$  are all the low-frequency coordinates  $q_3 \dots q_6$  and  $r$  the HF bond lengths ( $r_I$  and  $r_{II}$ ). The  $\phi_n$  are solu-

tions of the ‘‘clamped  $q$ ’’ Hamiltonian

$$\hat{H}(q, r) \phi_n(q, r) = V_n(q) \phi_n(q, r). \quad (19)$$

These define effective potentials  $V_n(q)$  for the combined stretching quantum states  $n \equiv \{\nu_I, \nu_{II}\} = \{\nu_1, \nu_2\}$ , where the former is an unsymmetrical combination of HF units, whereas the latter is essentially the combination of quantum numbers  $\nu_1$  and  $\nu_2$  used for (HF)<sub>2</sub>. The complete solution is

$$[\hat{T}_q + V_n(q)] \xi_{nm}(q) = E_{nm}^0 \xi_{nm}(q). \quad (20)$$

Tunneling can be calculated on these effective potentials by obtaining the  $E_{nm}^0$  and  $\xi_{nm}$ . Mills has discussed diagonal non Born–Oppenheimer corrections [94]. Predissociation will be mediated by off-diagonal nonadiabatic corrections  $\hat{H}_1$  in eq. (16), which are perfectly similar to the vibrationally nonadiabatic couplings discussed for vibrational redistribution [92,79]. Whereas some aspects of (HF)<sub>2</sub> dynamics can be described by both the crude adiabatic and the adiabatic picture, the latter will be more accurate, in general. We note that the original ideas of Stepanov [4] concerning hydrogen bonds would be consistent with both pictures and thus would not distinguish between them. We shall summarize some of our conclusions obtained in this conceptual framework.

## 5. Conclusions and outlook

(i) The HF stretching fundamentals and overtones (to  $N=4$ ) show sharp, line-like structures which provide information on predissociation lifetimes and rearrangement tunneling processes.

(ii) The rearrangement tunneling rates depend in a highly mode selective way upon the energy distribution over low- and high-frequency modes. The mode  $\nu_5$  promotes tunneling most effectively followed by  $K_a$  rotation and out of plane bending  $\nu_6$ . The (HF) stretching modes slow down rearrangement. This can be interpreted by an adiabatic separation of high- and low-frequency modes and effective vibrationally adiabatic potentials with increased barriers for rearrangement, although there are alternative descriptions.

(iii) Several experimental observations are consistent with a tightening up of (HF)<sub>2</sub> and increased hy-

drogen bonding when exciting (HF) stretching vibrations: (a) The trend of *A* and *B* rotational constants, (b) the hot band structure shifted  $9\text{ cm}^{-1}$  to high wavenumbers compared to the  $\nu_1$  fundamental, (c) the decreasing tunneling splittings upon  $\nu_1$  and  $\nu_2$  excitation.

A prediction from this conclusion would be an increased effective dissociation energy  $D_0(\nu_1 \text{ or } \nu_2)$  (cf. fig. 16), when increasing  $\nu_1$  or  $\nu_2$ . This prediction might be checked by considering predissociation widths of combination transitions near  $5000\text{ cm}^{-1}$ , which should show a sharp transition from line-like to broad structure by a change of predissociation mechanism. The relevant bands are too weak for this prediction to have been checked, so far.

(iv) The lifetimes inferred from the fundamental and overtone transitions of the (HF) stretching vibrations are very long and inconsistent with even the most extreme, tight RRKM or RRK models for unimolecular dissociation. This can be understood by a very weak non-adiabatic vibrational redistribution coupling between the high- and low-frequency modes in (HF)<sub>2</sub>, as it has also been found already in a different context for the high-frequency CH stretching mode in substituted acetylenes and other dynamical systems [90–92]. Density of states arguments exclude, however, that the observed spectral linewidths correspond only to the initial “redistribution” or internal conversion process for the fundamental and first overtones. Simplified coupled channel calculations using the artificial channel method are reasonably consistent with experiment [72–74].

Our results contribute towards a better understanding of the dynamics of hydrogen bonding in one of the most fundamental systems, perhaps the one most amenable to detailed theoretical understanding. Within the limitations inherent in the FTIR technique, the present data pave the way for a more detailed investigation of specific spectral regions by laser and molecular beam methods. The low-frequency rovibrational levels still need careful investigation. It also becomes increasingly clear that improved interaction potentials should be devised and vibrational variational calculations carried out in order to establish and understand the bound states with better accuracy. The theory of high vibrational states and predissociation rates will require simplified treatments, such as vibrationally adiabatic models.

Work in these directions is in progress [102].

### Acknowledgement

Substantial help from and discussions with Martin Suhm are gratefully acknowledged. René Gunzinger and E. Peyer helped building the equipment and H. Hollenstein and U. Schmitt contributed on various other aspects. I. Lippai edited the manuscript. Z. Al-Shamery helped drawing figures. We enjoyed correspondence with P.R. Bunker, N. Halberstadt, R.E. Miller, W. Lafferty, H. Lischka, A. Pine, M. Shapiro, and R.O. Watts. Our work is supported financially by the Schweizerischer Nationalfonds and the Schweizerischer Schulrat.

### References

- [1] P. Schuster, G. Zundel and G. Sandorfy, eds., *The Hydrogen Bond—Recent Developments in Theory and Experiments* (North-Holland, Amsterdam, 1976); P. Schuster, ed., *Hydrogen Bonds, Topics Current Chem.* 120 (1984).
- [2] G.C. Pimentel and A.L. McClellan, *The Hydrogen Bond* (Freeman, San Francisco, 1960).
- [3] N. Sheppard, in: *Hydrogen Bonding*, ed. D. Hadzi (Pergamon Press, New York, 1959) p. 85; E. Honegger and S. Leutwyler, *J. Chem. Phys.* 88 (1988) 2582; E. Honegger, R. Bombach and S. Leutwyler, *J. Chem. Phys.* 85 (1986) 1234; D.F. Coker and R.O. Watts, *Mol. Phys.* 58 (1986) 1113; M.A. Suhm, *Vibrational States of Water Clusters*, Internal Report ANU (Canberra, 1986).
- [4] B.I. Stepanov, *Nature* 157 (1946) 808.
- [5] G. Herzberg, *Molecular Spectra and Molecular Structure*, Vol. 3. *Electronic Spectra and Electronic Structure of Polyatomic Molecules* (Van Nostrand, Princeton, 1966).
- [6] M. Quack and J. Troe, *Theoretical Chemistry, Advances and Perspectives*, Vol. 6B, ed. D. Henderson (Academic Press, New York, 1981) p. 199.
- [7] *Faraday Discussion Chem. Soc.* 73 (1982) (on van der Waals Molecules); *Chem. Rev.* 88 (1988) 813 (on van der Waals Interactions).
- [8] M. Quack and J. Troe, in: *Gas Kinetics and Energy Transfer*, Vol. 2, eds. P.G. Ashmore and R.J. Donovan (The Chemical Society, London, 1977) p. 175.
- [9] J. Manz, in: *Molecules in Physics, Chemistry and Biology*, Vol. 3, ed. J. Maruani (Kluwer, Deventer, 1989) p. 365.
- [10] M. Quack, *Il Nuovo Cimento* 38 (1981) 358.

- [11] R.M. Badger and S.H. Bauer, *J. Chem. Phys.* 5 (1937) 839; R. Mecke, *Discussions Faraday Soc.* 9 (1950) 161; C.M. Huggins and G.C. Pimentel, *J. Phys. Chem.* 60 (1956) 161.
- [12] R.D. Hunt and L. Andrews, *J. Chem. Phys.* 82 (1985) 4442.
- [13] F.G. Celli and K.C. Janda, *Chem. Rev.* 86 (1986) 507.
- [14] R.L. Redington and D.F. Hamill, *J. Chem. Phys.* 80 (1984) 2446.
- [15] E. Knözinger and O. Schrems, in: *Vibrational Spectra and Structure*, Vol. 16, ed. J.R. Durig (Elsevier, Amsterdam, 1987) p. 142; C. Sandorfy, *Topics Current Chem.* 120 (1984) 42.
- [16] S. Bratoz and D. Hadzi, *J. Chem. Phys.* 27 (1957) 991; C.G. Cannon, *Spectrochim. Acta* 10 (1958) 341.
- [17] D.F. Smith, *J. Chem. Phys.* 48 (1968) 1429; *J. Mol. Spectry.* 3 (1959) 473.
- [18] P.V. Huong and M. Couzi, *J. Chim. Phys.* 66 (1969) 1309.
- [19] L. Andrews, V.E. Bondybey and J.H. English, *J. Chem. Phys.* 81 (1984) 3452.
- [20] L. Andrews and G.L. Johnson, *Chem. Phys. Letters* 96 (1983) 133.
- [21] W. Strohmeier and G. Briegleb, *Z. Elektrochem.* 57 (1953) 662, 668.
- [22] E.U. Franck and F. Meyer, *Z. Elektrochem.* 63 (1959) 571.
- [23] W. Klemperer, *Ber. Bunsenges. Physik. Chem.* 78 (1974) 128.
- [24] T.R. Dyke, B.J. Howard and W. Klemperer, *J. Chem. Phys.* 56 (1972) 2442.
- [25] B.J. Howard, T.R. Dyke and W. Klemperer, *J. Chem. Phys.* 81 (1984) 5417.
- [26] A.E. Barton and B.J. Howard, *Faraday Discussions Chem. Soc.* 73 (1982) 45.
- [27] H.S. Gutowsky, C. Chuang, J.D. Keen, T.D. Klots and T. Emilsson, *J. Chem. Phys.* 83 (1985) 2070.
- [28] W.J. Lafferty, R.D. Suenram and F.J. Lovas, *J. Mol. Spectry.* 123 (1987) 434.
- [29] T.R. Dyke, *Topics Current Chem.* 120 (1984) 85.
- [30] A.S. Pine and W.J. Lafferty, *J. Chem. Phys.* 78 (1983) 2154.
- [31] A.S. Pine, W.J. Lafferty and B.J. Howard, *J. Chem. Phys.* 81 (1984) 2939.
- [32] A.S. Pine and B.J. Howard, *J. Chem. Phys.* 84 (1986) 590.
- [33] A.S. Pine and G.F. Fraser, *J. Chem. Phys.* 89 (1988) 6636, 100.
- [34] J.L. Himes and T.A. Wiggins, *J. Mol. Spectry.* 40 (1971) 418.
- [35] J.M. Lisy, A. Tramer, M.F. Vernon and Y.T. Lee, *J. Chem. Phys.* 75 (1981) 4733.
- [36] M.F. Vernon, J.M. Lisy, D.J. Krajnovitch, A. Tramer, H.S. Kwok, Y.R. Shen and Y.T. Lee, *Faraday Discussions Chem. Soc.* 73 (1982) 387; D.W. Michael and J.M. Lisy, *J. Chem. Phys.* 85 (1986) 2528.
- [37] R.L. De Leon and J.S. Muentzer, *J. Chem. Phys.* 80 (1984) 6092.
- [38] Z.S. Huang, K.W. Jucks and R.E. Miller, *J. Chem. Phys.* 85 (1986) 3338.
- [39] K.W. Jucks and R.E. Miller, *J. Chem. Phys.* 86 (1987) 6637.
- [40] D.C. Dayton, K.W. Jucks and R.E. Miller, *J. Chem. Phys.* 90 (1989) 2631; K.W. Jucks and R.E. Miller, *J. Chem. Phys.* 88 (1988) 6059.
- [41] R.E. Miller, *Advan. Laser Sci.* 3 (1988) 365.
- [42] K. von Puttkamer, M. Quack and M.A. Suhm, *Mol. Phys.* 65 (1988) 1025.
- [43] K. von Puttkamer, M. Quack and M.A. Suhm, *Infrared Phys.* 29 (1989) 535.
- [44] K. von Puttkamer and M. Quack, *Mol. Phys.* 62 (1987) 1047.
- [45] K. von Puttkamer and M. Quack, *Chimia* 39 (1985) 358; *Proceedings of the 10th International Conference on Molecular Energy Transfer COMET 10* (1987) 195.
- [46] K. von Puttkamer and M. Quack, *Faraday Discussions Chem. Soc.* 82 (1986) 377.
- [47] K.D. Kolenbrander, C.E. Dykstra and J.M. Lisy, *J. Chem. Phys.* 88 (1988) 5995.
- [48] B.J. Dalton and P.D. Nicholson, *Intern. J. Quantum Chem.* 9 (1975) 325.
- [49] J.T. Hougen, in: *Structure and Dynamics of Weakly Bound Molecular Complexes*, ed. A. Weber, *NATO ASI Series* (Reidel, Dordrecht, 1987) p. 191.
- [50] J.T. Hougen and N. Ohashi, *J. Mol. Spectry.* 109 (1985) 134.
- [51] M. Kofranek, H. Lischka and A. Karpfen, *Chem. Phys.* 121 (1988) 137.
- [52] P.R. Bunker, M. Kofranek, H. Lischka and A. Karpfen, *J. Chem. Phys.* 89 (1988) 3002.
- [53] P.R. Bunker, T. Carrington, P.C. Gomez, M.D. Marshall, M. Kofranek, H. Lischka and A. Karpfen, *J. Chem. Phys.*, in press.
- [54] H. Lischka, *Chem. Phys. Letters* 66 (1979) 108; *J. Am. Chem. Soc.* 96 (1974) 4761.
- [55] D.W. Schwenke and D.G. Truhlar, *J. Chem. Phys.* 88 (1988) 4800.
- [56] G.C. Hancock, D.G. Truhlar and C.E. Dykstra, *J. Chem. Phys.* 88 (1988) 1786; G.C. Hancock and D.G. Truhlar, *J. Chem. Phys.* 90 (1989) 3498.
- [57] D.W. Michael, C.E. Dykstra and J.M. Lisy, *J. Chem. Phys.* 81 (1984) 5998; C.E. Dykstra, *Chem. Phys. Letters* 141 (1987) 159.
- [58] A. Beyer and A. Karpfen, *Chem. Phys.* 64 (1982) 343.
- [59] A.E. Reed, F. Weinhold, L.A. Curtiss and D.J. Pochatko, *J. Chem. Phys.* 84 (1986) 5687.
- [60] C. Amovilli and R. McWeeny, *Chem. Phys. Letters* 128 (1986) 11.
- [61] D.R. Yarkony, S.V. O'Neill, H.F. Schaefer III, C.P. Baskin and C.F. Bender, *J. Chem. Phys.* 60 (1974) 855; P. Bouchez, R. Block and L. Jansen, *Chem. Phys. Letters* 65 (1979) 212;

- J.F. Gaw, Y. Yamaguchi, M.A. Vincent and H.F. Schaefer III, *J. Am. Chem. Soc.* 106 (1984) 3133.
- [62] L.A. Curtiss and J.A. Pople, *J. Mol. Spectry.* 61 (1976) 1.
- [63] M.J. Frisch, J.E. Del Bene, J.S. Binkley and H.F. Schaefer III, *J. Chem. Phys.* 84 (1986) 2279.
- [64] M.M. Chase Jr., J.L. Curnett, J.R. Downey Jr., R.A. McDonald and A.N. Syverud, *J. Phys. Chem. Ref. Data* 11 (1982) 635.
- [65] J.P. Toennies, M. Mann, K. Müller, E.L. Knuth and J.B. Fenn, *Proc. 14th Symp. Rarefield Gas Dynamics* (1984) 733;  
H.G. Rubahn, J.P. Toennies, M. Wilde and J. Wanner, *Chem. Phys. Letters* 120 (1985) 11.
- [66] J.A. Beswick and J. Jortner, *J. Chem. Phys.* 68 (1978) 2277.
- [67] G.E. Ewing, *J. Chem. Phys.* 72 (1980) 2096; 71 (1979) 3143; *Chem. Phys.* 29 (1978) 253; 63 (1981) 411.
- [68] G. Henderson and G.E. Ewing, *Mol. Phys.* 27 (1974) 903.
- [69] D.S. Anex, E.R. Davidson, C. Douketis and G.E. Ewing, *J. Phys. Chem.* 92 (1988) 2913.
- [70] G.E. Ewing, *J. Phys. Chem.* 91 (1987) 4662; *Faraday Discussions Chem. Soc.* 73 (1982) 325.
- [71] C.A. Coulson and G.N. Robertson, *Proc. Roy. Soc. A* 342 (1975) 289.
- [72] N. Halberstadt, Ph. Bréchnac, J.A. Beswick and M. Shapiro, *J. Chem. Phys.* 84 (1986) 170.
- [73] N. Halberstadt, private communication; Thèse, Université de Paris-Sud, Orsay, France (1987).
- [74] M. Shapiro and R. Bersohn, *Ann. Rev. Phys. Chem.* 33 (1982) 409.
- [75] H. Meyer, E.R.T. Kerstel, D. Zuang and G. Scoles, *J. Chem. Phys.* 90 (1989) 4623.
- [76] S.G. Lieb and J.W. Bevan, *Chem. Phys. Letters* 122 (1985) 284.
- [77] K.C. Janda, *Photodissociation Photoionization*, ed. K.P. Lawley (Wiley, New York, 1985).
- [78] D.A. Dixon, D.R. Herschbach and W. Klemperer, *Faraday Discussions Chem. Soc.* 62 (1977) 341.
- [79] H.R. Dübal and M. Quack, *J. Chem. Phys.* 81 (1984) 3779.
- [80] M. Lewerenz and M. Quack, *J. Chem. Phys.* 88 (1988) 5408.
- [81] G. Guelachvili, *Opt. Commun.* 19 (1976) 150.
- [82] U.K. Sengupta, P.K. Das and K. Narahari Rao, *J. Mol. Spectry.* 74 (1979) 322.
- [83] E.S. Fishburne and K. Narahari Rao, *J. Mol. Spectry.* 19 (1966) 290.
- [84] R.N. Spanbauer, K. Narahari Rao and L.H. Jones, *J. Mol. Spectry.* 16 (1965) 100.
- [85] J.W.C. Johns and R.F. Barrow, *Proc. Roy. Soc. A* 251 (1959) 504.
- [86] G.A. Baker Jr., *Essentials of Padé Approximants* (Academic Press, New York, 1975).
- [87] S. Liu and C.E. Dykstra, *J. Phys. Chem.* 90 (1986) 3097.
- [88] A. Campargue, F. Stoeckel, M. Chenevier and H. Ben Kraiem, *J. Chem. Phys.* 87 (1987) 5598.
- [89] M.-C. Chuang, J.E. Baggott, D.W. Chandler, W.E. Farneth and R.N. Zare, *Faraday Discussions Chem. Soc.* 75 (1983) 301.
- [90] M. Quack, *Far. Discussions Chem. Soc.* 71 (1981) 309.
- [91] K. von Puttkamer, H.R. Dübal and M. Quack, *Faraday Discussions Chem. Soc.* 75 (1983) 197;  
H.R. Dübal and M. Quack, *Chem. Phys. Letters* 90 (1982) 370.
- [92] T. Carrington, *J. Chem. Phys.* 86 (1987) 2207.
- [93] C.S. Parmenter, *Faraday Discussions Chem. Soc.* 75 (1983) 7.
- [94] I.M. Mills, *J. Phys. Chem.* 88 (1984) 532;  
E.L. Sibert, *J. Phys. Chem.* 93 (1989) 5022.
- [95] M. Quack and J. Troe, *Ber. Bunsenges. Physik. Chem.* 78 (1974) 240.
- [96] G.T. Fraser, *J. Chem. Phys.* 90 (1989) 2097.
- [97] M. Quack and J. Troe, *Ber. Bunsenges. Physik. Chem.* 79 (1975) 170.
- [98] J. Jortner, S.A. Rice and R.M. Hochstrasser, *Advan. Photochem.* 7 (1969) 149.
- [99] F.H. Mies and M. Krauss, *J. Chem. Phys.* 45 (1966) 4455;  
F.H. Mies, *J. Chem. Phys.* 51 (1969) 787, 798.
- [100] T. Beyer and D.F. Swinehart, *Commun. ACM* 16 (1973) 379;  
S.F. Stein and B.S. Rabinovitch, *J. Chem. Phys.* 58 (1973) 2438.
- [101] M. Quack, *J. Chem. Phys.* 82 (1985) 3277.
- [102] M. Quack and M.A. Suhm, *Proceedings of the 11th Colloquium on High Resolution Molecular Spectroscopy, Giessen 1989, and to be published.*